American Journal of Environmental Sciences

Original Research Paper

A Novel River Meander Migration and Cutoff Model: A New Perspective

Youssef Ismail Hafez

Private Consultant and Former Professor at Nile Research Institute, Delta Barrage, El Qanater, Greater Cairo, Egypt

Article history
Received: 17-07-2024
Revised: 11-09-2024
Accepted: 20-11-2024

Email: youssefhafez995@gmail.com

Abstract: Accurate prediction of river meander migration is crucial for effective river management and operation, particularly in light of climate changes and human-induced interventions. Existing models often rely on single-equation approaches, such as bank erosion rate versus excess bank velocity or excess bank shear stress, which limit their ability to comprehensively capture the complex dynamics of meander evolution. This study presents a novel two-equation model for predicting river meander migration, representing a significant advancement in the fields of geomorphology, hydrology and river engineering. The proposed model introduces two coupled equations that comprehensively determine the movement of a point on the channel centreline capturing both the change in the channel centerline radius of curvature (r) and the change in the arc angle (θ). This approach provides a more holistic representation of meander migration compared to previous methods, allowing for a better understanding of the underlying physical processes. Furthermore, the paper presents an equation to estimate the critical discharge required for the occurrence of neck and chute cutoffs at a meander bend, incorporating the influence of channel geometry and flow characteristics. This contribution enhances the understanding of the cutoff process and its implications for river morphology. To validate the effectiveness of the meander migration model, two distinct case studies are considered: (1) Prediction of thalweg wavelength meandering in the Nile River, Egypt, where the model successfully captured the observed meander characteristics, demonstrating its accuracy in predicting large-scale meander patterns; and (2) Determination of river channel radius of curvature in four rivers in Texas, USA, where the model accurately predicted the radius of curvature in these diverse river systems, showcasing its applicability across different scales and environments. These results highlight the model's ability to accurately predict meander migration and cutoff events, making it a valuable tool for river management and planning.

Keywords: River Meander Migration, Meander Neck-Cutoff and Chute Cutoff, Excess Energy Theory, Energy Balance Theory, Response Theory For River Adjustment, Nile River (Egypt), Four Texas Rivers (USA)

Introduction

Throughout history, rivers have served as vital habitats for various aquatic organisms and wildlife such as fish, aquatic plants and aquatic birds. In addition rivers have been attractive locations for human settlements and civilizations, drawing people to live along their flood plains. However, the dynamic nature of rivers influenced by factors such as floods, droughts and the effects of global warming and climate change, leads to constant evolution and movement of river channels over time. Rivers exhibit lateral and downstream/upstream shifts, resulting in changes to their plan form, including the straightening of curved reaches (meander cut-off or meander decay) or the increasing curvature of meanders meander growth. These lateral shifts or contractions of river channels have significant impacts on river banks, flood plains and the surrounding environment, including existing structures such as river bridge crossings, intake water plants, roads, agricultural lands and buildings. The potential threats

posed by river shifting, shrinking and lateral movements necessitate a deep understanding and accurate prediction of river channel meandering evolution.

In their study Briaud *et al*. (2001) highlight that rivers are dynamic systems where the flow of water can alter the elevation and lateral position of the riverbed and riverbanks. Meanders, in particular, are susceptible to changes in lateral location due to the centrifugal force that increases shear stress at the interface between water and soil. Predicting the movement of meanders is both challenging and crucial as such movements can lead to costly maintenance issues for nearby bridges. Briaud *et al*. (2001) provide an example from the Brazos River near Navasota, Texas, where a meander shifted over 300m towards a bridge abutment between 1910 and 1981, while another meander further downstream moved over 200m towards the Navasota River during the same period. Therefore, understanding and predicting the formation and ongoing processes of river channel meandering evolution are of paramount importance for efficient and successful river management, operation, protection and control.

Existing models for predicting river meander migration often rely on single-equation approaches, such as bank erosion rate versus excess bank velocity or excess bank shear stress, which limit their ability to comprehensively capture the complex dynamics of meander evolution. This study presents a novel two-equation model for predicting river meander migration, representing a significant advancement in the field. Furthermore, the paper presents an equation to estimate the critical discharge required for the occurrence of neck and chute cutoffs at a meander bend, incorporating the influence of channel geometry and flow characteristics. This contribution enhances the understanding of the cutoff process and its implications for river morphology.

Review of Existing Works

Existing research on river meandering can be classified into several categories. First, there are empirical equations and regression-based equations that describe the plan form of river meanders, such as the regime theory geomorphic equations proposed by Leopold and Wolman (1960), Howard and Hemberger (1991), and Finotello *et al*. (2020). Second, various theories and doctrines have been put forth to explain and describe river meanders. For example, Leopold and Langbein (1966) suggested that meanders appear in the form that minimizes the work done by the river in turning, while Langbein and Leopold (1966) presented the theory of minimum variance, where a stream adjusts to increasing discharge by minimizing the total variance of its dependent variables. Other theories attribute meandering to perturbations in turbulent flows (Yalin, 1971), the growth and decay of secondary currents (Chang, 1984), the action of horizontal turbulence bursts on deformable banks (Da Silva, 2006), or excess energy (Hafez, 2022). Third, there are empirical equations that model meander migration, including the approaches proposed by Keady and Priest (1977); Hooke (1980); Brice (1982); Nanson and Hickin (1983). Fourth, time-sequence maps and extrapolation approaches have been used to study meander migration (Brice, 1982; Lagasse, 2001). Fifth, several meander migration models have been developed by researchers such as Ikeda *et al*. (1981); Howard and Knutson (1984); Seminara *et al*. (2001); Abad and Garcia (2006); Seminara (2006); Camporeale *et al*. (2007); Frascati and Lanzoni (2009); Pittaluga and Seminara (2011); Schwenk *et al*. (2015); Bogoni *et al*. (2017); Monegaglia and Tubino (2019). Finally, there is work specifically focused on meander cutoff, a complex process that involves factors such as the material composition of the riverbank, changes in incoming water and sediment, boundary conditions and vegetation (Hooke, 2004; Constantine *et al*., 2010; van Dijk *et al*., 2012; Ielpi *et al*., 2021; Wu *et al*., 2023).

The first two categories, empirical approaches and theories on river meandering, have been extensively discussed in Hafez (2022). This study primarily focuses on meander migration analytical modeling, presenting relevant findings from both empirical and theoretical approaches to meandering. Meander cutoff is briefly addressed as a highly complex process that warrants separate analysis and is beyond the scope of this study. The factors influencing cutoff in natural rivers are multifaceted, including the composition of riverbanks, changes in water and sediment inputs, boundary conditions and vegetation (Wu *et al*., 2023).

Regarding meander migration, Monegaglia and Tubino (2019) argue that the geometry of the bankfull channel should change during the planform evolution of a meandering river for two main reasons. First, the elongation of a channel connecting two floodplain points leads to a subsequent reduction in channel slope (Zolezzi *et al*., 2009; Eke *et al*., 2014). Second, any variation in local slope triggers a counteracting mechanism resulting from the imbalance between sediment supply and sediment transport capacity. Blanckaert (2011) further emphasizes that the migration rate of meanders depends on multiple parameters, including the meander planform (which defines the evolution of centerline radius of curvature, width and influences of upstream and downstream bends), average flow depth, sediment characteristics, bank erodibility and roughness. The occurrence of channel straightening in a meander reach can be attributed to a change in fluvial style, marked by a significant increase in the wavelength towards a straight channel path, or through cutoff processes (such as neck cutoff or chute cutoff) depending on the relative magnitudes of the variables (Hafez, 2022).

In the field of river meander migration, various models have been developed to study the complex processes of bank erosion and channel evolution. One influential model

introduced by Ikeda *et al*. (1981) presents a morphodynamic approach to bank erosion in sinuous channels. This model describes the lateral migration rate, denoted as ζ, at a point along the channel centerline. It is defined as the product of a bank erodibility coefficient, E_0 and an excess bank velocity, U_b, which arises from perturbations in channel curvature and bar formation (Eq. 1):

$$\zeta = E_0 U_b \quad (1)$$

The excess bank velocity represents the difference between the depth-averaged near-bank velocity and the cross-sectionally averaged velocity.

The work of Ikeda *et al*. (1981) has served as a source of inspiration for subsequent studies on meandering migration, with researchers such as Seminara *et al*. (2001); Seminara (2006); Camporeale *et al*. (2007); Frascati and Lanzoni (2009); Pittaluga and Seminara (2011); Ashraf and Liu (2013); Monegaglia and Tubino (2019) adopting and building upon their approach. However, Hafez (2022) points out a limitation of this model, namely that it requires an initial flow curvature or perturbation for sustained meandering. Linear stability theory for finite domains confirms the need for continuous perturbations for sustained meandering, Weiss *et al.* (2022).

To model the lateral rate of hydraulic erosion, Motta *et al*. (2012) introduced Eq. (2), which relates the erosion rate, E*, to the excess shear stress in each bank-material layer:

$$E^* = M^* \left({}^{\tau^*}/_{\tau_c^*} - 1 \right) \quad (2)$$

The erosion-rate coefficient, M* and the critical shear stress, τ_c*, are key parameters in this relation. While the bank shear stress $\tau^*$is assumed to be equal to the near-bank bed shear stress predicted by a hydrodynamic model. Hafez (1995) showed significant differences between the bed and bank shear stresses using the two-equation (κ-ε) non-linear turbulence hydrodynamic model. Zhao *et al*. (2021) adopted Eq. (2) for bank erosion, but employed a different equation for bank accretion, introducing proportionality coefficients to probabilistically constrain channel width variations.

Abad and Garcia (2006) developed the River Restoration Toolbox (RVR), a toolbox for simulating river meander migration based on physically based bank erosion methods. RVR Meander offers two methods for computing the river centerline migration: A classic approach based on near-bank excess velocity multiplied by a river migration coefficient and a physically based approach that accounts for fluvial erosion driven by exceedance of a critical shear stress and mass soil structure failure. However, the RVR model has certain limitations, including the use of a constant water discharge, neglect of bed aggradation or degradation, assumption of constant channel width, omission of cutoff processes and the constant application of specified parameters over time, which may not account for natural or man-made perturbations.

While numerical models, including meander-dynamics models, are valuable tools for studying river meandering, their reliability depends on the availability of sufficient data for calibration. Typically, calibration involves adjusting soil parameters, such as the erosion-rate coefficient or the soil critical shear stress, to match known historic river centerlines with recent ones. The calibration process requires extensive flow data over long time periods, which may not always be readily available.

Meander-dynamics models are commonly employed to investigate the long-term dynamics of river meandering over hundreds, if not thousands, of years. For instance, Schwenk *et al*. (2015) conducted a simulation spanning 30,000 years to study the life cycle of a meander bend, while Camporeale *et al*. (2007) simulated meander evolution over a period of 3,000 years. However, these models heavily rely on data availability for calibration, posing a challenge when such data is not accessible (Hafez, 2022). In such cases, the reliability of these models diminishes and alternative approaches become necessary to predict the final equilibrium geometry of river meanders. The present approach stands out as one of the few viable options in such scenarios.

Furthermore, existing models predominantly focus on bank erosion conditions but often overlook bank deposition processes, employing the same bank erosion coefficient (denoted as E_o or M*) without accounting for a separate coefficient to represent bank accretion. For instance, Monegaglia and Tubino (2019), whose meander migration model is similar to Eq. (1), assume that their bank migration equation implicitly assumes a certain rate of bank shifting scaled by the coefficient E_o, regardless of whether the bank is retreating or advancing. Similarly, Zhao *et al*. (2021) set both the erosion and deposition coefficients (in m/s) to 1×10^{-6} m/s. The erosion coefficient essentially acts as a placeholder for unknown physics and includes numerical aspects of the meander model implementation, making it a "fudge factor" in practice (Crosato, 2007).

It is worth noting that in these models, the local migration rate is calculated perpendicular to the centerline direction (Sylvester *et al*., 2019; Zhao *et al*., 2021). The Ikeda *et al*. (1981) relation assumes that rivers migrate to maintain constant bankfull channel width, but does not provide underlying physics to support this assumption. Parker *et al*. (2011) question the validity of this assumption, particularly concerning the synchronization of inner-bank depositional processes with outer-bank erosional processes.

The application of the meander migration model proposed by Ikeda *et al*. (1981) to real river cases has raised concerns regarding its accuracy and reliability. This issue is exemplified by the study conducted by Ashraf and Liu (2013), who utilized the RVR meander package

DOI: 10.3844/ajessp.2025.12.38

incorporating Ikeda *et al*. model (Eq.1). They aimed to calibrate the model by estimating the bank erosion coefficient (E_o) using four rivers in Texas, USA: The Brazos River, Nueces River, Sabine River and Trinity River. The calibration process involved determining E_o based on historical planform changes and measured long-term migration rates.

The calibration results revealed significant prediction errors, measured as the ratio of the area between simulated and observed centerlines to the length of the observed centerline. The Nueces River exhibited prediction errors ranging from 29.51-91.58 m, while the Brazos River showed errors ranging from 39.28-41.85 m. The Sabine River had errors ranging from 41.7-130.87 m and the Trinity River had errors ranging from 42.38-84.11 m. Moreover, the erosion coefficient varied not only between different rivers but even within the same river bend, exhibiting a wide range of values. For instance, in the Sabine River, the erosion coefficient varied from $3.66*10^{-8}$-$1.43*10^{-7}$, representing a four-fold difference.

Interestingly, when Ashraf and Liu (2013) ran the model for different projection years using the minimum calibrated projection error coefficients, they obtained projection errors ranging from 0.11-0.26 times the channel width. The channel widths ranged from 129-171 m. Typically, the errors in the calibration process are expected to be smaller than in the verification process. However, in the case of Ashraf and Liu's application of Ikeda *et al*. model to the four USA Rivers in Texas, this was not the observed pattern.

To assess the precision and accuracy of various river migration prediction equations, Briaud *et al*. (2001) conducted a study using six case histories from four rivers in Texas, USA: The Brazos River, Nueces River, Trinity River and Guadalupe River. They evaluated prediction methods such as the Keady and Priest (1977) approach, the Hooke (1980) approach, the Brice (1982) approach, the Nanson and Hickin (1983) approach and the time-sequence maps and extrapolation approach (Brice, 1982; Lagasse, 2001). The results showed that the Keady and Priest method was reasonably conservative, the Hooke method appeared overly conservative, the Brice method significantly underpredicted the measurements and the Nanson and Hickin method yielded mixed results.

In summary, meander migration models play a crucial role in understanding the complex processes of river bank erosion and channel evolution. However, these models often rely on field data calibration and have limitations in terms of data availability and accuracy. The bank erosion coefficient and its relationship to water discharge and sediment load remain important considerations. Improving the reliability and accuracy of meander migration models requires further research and development to better capture the underlying physics and dynamics of bank erosion and deposition processes.

Some researchers have employed minimization concepts of energy-related quantities to determine channel geometry, including plan form geometry. For example, Yang *et al*. (1981) used the unit stream power, Chang (1992) utilized stream power, Yalin (1992) employed the flow Froude number and Yalin and Da Silva (2001) utilized average velocity. Hafez (2000; 2001a-b; 2002) applied extremal methods to quantify changes in flow discharges and sediment loads for determining the geometry of straight alluvial river reaches. He employed a direct variational or extremal approach, which avoids the complexities associated with minimization techniques and computer programming. This approach will be utilized in the current study. The following paragraphs are going to discuss the direct variational or extremal approach by Hafez (2000).

Hafez (2000) introduced a response theory that predicts the direction and magnitude of adjustments in alluvial rivers when transitioning from one regime to another. The theory is based on the tendency of alluvial channels to reach dynamic equilibrium after being disturbed by extreme conditions such as floods or dam construction or meander cutoff. Various extremal concepts are employed, including energy dissipation (such as stream power, unit stream power and energy slope), sediment efficiency, friction factor and Froude number. Initially, the theory focused on straight river sections and later expanded to incorporate additional extremal concepts, such as the extremal boundary shear stress (Hafez, 2001a), the effects of sediment loads on stream geometry (Hafez, 2001b) and the effects of water discharge and sediment changes on hydraulic geometry exponents (Hafez, 2002). The hydraulic exponents of the regime theory, which are typically considered constants, are derived in a more general manner that encompasses the classical reported values as shown in Hafez (2000; 2002).

The response river theory, Hafez (2000), is described in detail herein due to its relevance to the current study. The theory is based on the following assumptions: (1) A rectangular and one-dimensional analysis, (2) A straight and wide channel, (3) At-a-station hydraulic geometry analysis and (4) First-order variations of the variables.

The equilibrium conditions of a river channel depend on various factors, including channel discharge, roughness measure, energy slope, width, depth, sediment discharge and bed material size. Mathematically, this can be expressed as, Hafez (2000):

$$\Psi = \Psi\,(Q, \Phi, S, B, D, Q_s, D_s) \tag{3}$$

Here, Ψ represents a variable that describes the equilibrium conditions of the river, such as energy slope or stream power, Q is the flow discharge, Φ represents a measure of channel roughness, such as the Manning roughness coefficient or Darcy Weisbach friction factor. S is the energy slope, B is the average width of the reach, D

DOI: 10.3844/ajessp.2025.12.38

is the average depth, Q_s is the sediment discharge and D_s is a measure of bed material size. According to the response theory, if any of the variables in Eq. (3) change, the corresponding change in Ψ required to restore equilibrium should be zero, expressed as:

$$\Delta\Psi = \sum_i \left(\frac{\partial\Psi}{\partial x_i}\right) \Delta x_i + H.O.T = 0. \quad (4)$$

Here, x_i represents any of the variables on the right-hand side of Eq. (3), H.O.T. denotes higher-order terms and Δx_i represents the change in the variable relative to its original value. For example, $\Delta x_i = x_2 - x_1$, where x_2 is the value of the variable after an excitation, such as a flood or dam and x_1 is the value before the excitation.

An equivalent linear form of Eq. (4) is:

$$\frac{\Delta\Psi}{\Psi} = 0 \quad (5)$$

Equations (4-5) is the general equation corresponding to an extremal condition (either maximum or minimum) of the function describing the equilibrium conditions of the river channel. This function can be stream power, energy slope, friction factor, sediment transport, or Froude number.

The application of Eq. (5) according to Hafez (2000) is demonstrated to predict changes in width, depth and slope in straight reaches. For a very wide channel, the Darcy-Weisbach friction factor is well known to be expressed as:

$$f = \frac{8\, g\, D^3\, S\, B^2}{Q^2} \quad (6)$$

Here, f represents the friction factor, g is the gravitational acceleration and all variables are assumed to be reach averages.

To determine extremal conditions for the friction factor which means that the river channel adjusts any or all of the variables in the right hand side of Eq. (6) to impose extreme value of the friction factor function, the variation of its function is set to zero, resulting in $\Delta f = 0$ or alternatively $\Delta f/f = 0$. This can be expressed mathematically as:

$$\Delta f = \frac{\partial f}{\partial D}\Delta D + \frac{\partial f}{\partial S}\Delta S + \frac{\partial f}{\partial B}\Delta B + \frac{\partial f}{\partial Q}\Delta Q \quad (7)$$

By applying Eq. (7) and Eqs. (5-6), the following equation is obtained (Hafez, 2000 for detailed derivation):

$$3\,\frac{\Delta D}{D} + \frac{\Delta S}{S} + \frac{\Delta B}{B} - 2\,\frac{\Delta Q}{Q} = 0 \quad (8)$$

Equation (8) in combination with flow continuity and flow resistance equations determine the adjustments in width, depth and slope of a river channel due to changes in flow discharge, assuming discharge is the only controlling or independent variable. The effects of sediment load discharge were later incorporated in Hafez (2001a-b). The response theory has been primarily applied to straight river reaches, but it will be herein extended to curved and meandering channels as well. Overall, Hafez's response theory provides a framework for predicting river adjustments based on extremal conditions and the concept of dynamic equilibrium. It considers various variables and their interactions to model the changes in width, depth and slope of alluvial rivers.

In Hafez's ground-breaking work in Hafez (2000), the response theory demonstrated its effectiveness in predicting a range of river adjustments in various locations around the world. For instance, the theory successfully predicted the width of the channel flood, as well as the depths of scour and deposition at the Basilone Road Bridge on the Santa Margarita River in California, USA, during the 1978 event. Similarly, it accurately estimated the channel bed scour caused by floods in the San Dieguito River at Santa Fe, California in both 1978 and 1980. Furthermore, the theory was able to accurately describe the breach morphology, including width and depth dimensions, at the San Diego River during the 1978 flood.

Additionally, the response theory proved its applicability to other scenarios. It successfully predicted the width changes in the stream-delta system of the San Elijo Lagoon resulting from the flushing event in 1975. The theory also accounted for the alterations in width caused by dam construction in rivers such as the Jemez River in New Mexico, the Arkansas River in Colorado and the Wolf Creek in Oklahoma, USA. It accurately captured the width adjustments resulting from the implementation of dam cut-offs in the Mississippi River, which led to significant changes from 1310 m in 1933 to approximately 2000 m in 1975. Additionally, the theory successfully accounted for width changes due to variations in slope at the Chippewa River in Wisconsin, USA.

Building on these achievements, Hafez's subsequent work in 2001 extended the application of the response theory to other notable cases. It accurately predicted the severe channel width change in the Santa Cruz River near Tucson, Arizona, caused by the 1983 flood. Furthermore, it successfully estimated the severe bed scour below Buford Dam on the Chattahoochee River in Georgia, USA.

The response theory also demonstrated its effectiveness in international contexts. Successful predictions were made regarding the channel width changes resulting from floods in the Yellow River in China. Moreover, the response theory was employed to examine changes in the width of the Nile River in Egypt, specifically in the reach upstream of Cairo, subsequent to the construction of the Aswan High Dam. Additionally the theory accurately captured the channel width adjustments due to dam construction in various rivers across the United States. Overall, Hafez's response theory has proven to be a

DOI: 10.3844/ajessp.2025.12.38

valuable tool in predicting and understanding river adjustments in different environments worldwide. Its ability to account for a wide range of factors and scenarios makes it a valuable contribution to the field of river engineering and geomorphology.

To incorporate sediment load effects on stream adjustments, Hafez (2001b) utilized the simplified sediment transport equation developed by Yang (1986). This equation expresses the stream power per unit weight, *QS* (where S represents the longitudinal slope), as follows:

$$Q\,S = \frac{1}{k}\,\frac{Q_s\,D_{50}^{0.5}\,B\,D}{Q} \tag{9}$$

Here, Q_s represents the bed material discharge, D_{50} denotes the median sediment size and k is a coefficient. By applying the extremal condition $\Delta(QS) / (QS) = 0$ to Eq. (9) and solving for the width term, the following result is obtained:

$$\frac{\Delta B}{B} = \frac{\Delta Q}{Q} - \frac{\Delta Q_s}{Q_s} - \frac{1}{2}\,\frac{\Delta D_{50}}{D_{50}} - \frac{\Delta D}{D} \tag{10}$$

With the inclusion of sediment load effects in Hafez (2001b), the unexpected case of an increase in channel width due to dam construction in the Missouri River, USA, was successfully predicted in terms of both direction and magnitude using Eq. (10).

In regime methods, channel width, depth and slope are expressed as functions of the channel forming discharge, often referred to as the bankfull discharge, as described by Lacey (1930, 1958); Leopold and Maddock (1953). These relationships were based on canals and rivers assumed to be in a regime or equilibrium state in India, Pakistan and the United States. The general form of these relationships is as follows:

$$B = a\,Q^b\,;D = c\,Q^f\,;V = e\,Q^m\,;S = i\,Q^j\,;and\;n = t\,Q^y \tag{11}$$

Here, *B* represents the channel top width, *D* is the average depth, *V* denotes the average velocity, *S* represents the channel longitudinal slope and *n* is the Manning's roughness coefficient. The coefficients *a, b, c, f, e, m, i, j, t* and *y* are empirical values determined through regression analysis of field data. Leopold and Maddock (1953), using 20 river cross-sections, reported mean values of "*b*" as 0.26, "*f*" as 0.4 and "*m*" as 0.34. Lacey (1930; 1958) determined "*b*" as 0.5 and "*j*" as -1/6 based on data from canals assumed to be in a regime state in India and Pakistan. Blench (1952; 1970), following Lacey's approach, determined "*b*" as 0.5, "*f*" as 1/3, "*m*" as 1/6 and "*j*" as -1/6. Simons and Albertson (1960), using canals in India, Pakistan and other locations in Colorado, Wyoming and Nebraska in the USA, determined "*b*" as 0.5 and "*f*" as 0.36.

Applying the response theory technique, as described in Eq. (5), to the relationships in Eq. (11) yields:

$$\frac{\Delta B}{B} = b\,\frac{\Delta Q}{Q}\,;\,\frac{\Delta D}{D} = f\,\frac{\Delta Q}{Q}\,;\,\frac{\Delta V}{V} = m\,\frac{\Delta Q}{Q};\,\frac{\Delta S}{S} = j\frac{\Delta Q}{Q};\;and\;\frac{\Delta n}{n} = y\,\frac{\Delta Q}{Q} \tag{12}$$

These relationships in Eq. (12) will be employed later in the present approach.

One of the regime relationships that describe the meander wavelength, λ, Fig. (1), in relation to discharge is proposed by Dury (1964) as follows:

$$\lambda = 54.3\,(Q_{ma})^{0.5} \tag{13}$$

Here, Q_{ma} represents the mean annual flood. Different researchers have obtained various coefficients in Eq. (13) depending on the definition of discharge, but the exponent value remains consistently around 0.5. For instance, Carlston (1965) reported 0.46, Ackers and White reported 0.47 and Dury (1976) reported 0.55. Yalin (1971) and Da Silva (2006) expressed the wavelength in terms of the channel width as follows:

$$\lambda = 2\,\pi\,B\;\approx 6\,B \tag{14}$$

The regime approach suggests that a single variable, such as discharge or width, is the sole controlling factor that influences channel adjustments.

Hafez (2022) conducted research on the causes of river meandering and proposed that the imbalance between the valley slope (S_V) and the regime channel slope (S_R) is the primary factor, assuming that the sediment load is below the transport capacity and the bank erodibility allows for meandering. The study suggested that when a river reach encounters a steep valley slope, it tries to maintain energy balance by dissipating the excess energy through channel curvature. Mathematically, this can be expressed as the difference between the valley slope and the regime channel slope, which equals the transverse energy loss slope:

$$S'' = S_V - S_R \tag{15}$$

where *S*" is the transverse energy slope due to curvature-induced energy loss, S_V is the steep valley slope and S_R is the relatively flat regime channel slope. Hafez (2022) expressed the regime slope (S_R) as a function of various parameters such as unit bed load discharge (q_s), median bed size (d_m), water unit weight (γ), channel hydraulic radius (*R*) and critical shear stress for incipient motion (τ_c). It should be noted that determining the regime channel slope (S_R) using a sediment transport formula can be challenging for specific river reaches. However, Hafez (2022) proposed a simpler and more direct approach, which will be explained in subsequent sections.

To estimate the transverse energy expenditure in curved reaches (*S*"), Hafez (2022) employed either Rozovskii (1957); Chang (1992) approach, in the following equation form:

$$S'' = \Phi(R)\left(\frac{D}{r}\right)^2 F_r^2 \quad (16)$$

Here, $\Phi(R)$ is a friction function, D represents the channel depth, r is the channel radius of curvature (approximated as the radius of the best-fit circle to the meander path), r is r_c in Fig. (1) and F_r is the Froude number. The friction function could be given either by Eqs. (17-18), respectively:

$$\Phi(f) = \frac{2.07\, f + 4.68\sqrt{f} - 1.83\, f^{3/2}}{0.565 + \sqrt{f}} \quad (17)$$

$$\Phi(C) = \left(12\,\frac{\sqrt{g}}{C} + 30\,\frac{g}{C^2}\right) \quad (18)$$

These functions depend on roughness parameters such as Chezy's roughness coefficient (C) or the Darcy-Weisbach friction factor (f) and are used to calculate the transverse energy expenditure.

By applying Eq. (15) and utilizing Eq. (16) for S'', Hafez (2022) derived Eq. (19) to predict the channel radius of curvature (r):

$$r = D\,F_r\sqrt{\frac{\Phi(f)}{(S_V - S_R)}} = D\,F_r\sqrt{\frac{\Phi(C)}{(S_V - S_R)}} \quad (19)$$

Hafez (2022) further considered that by applying Eq. (19) at two consecutive times (t_1 and t_2) and at a given point along the channel in the streamwise direction (at distance s), the change in the channel radius of curvature over time ($\Delta r(s)$) can be obtained. This change represents the development of meanders over time at a specific location, which is analogous to bank changes. For lateral meander migration, $\Delta r(s)$ also represents the shift of the lateral banks.

Ielpi *et al*. (2021) conducted an analysis of 227 meander cutoff events in the Humboldt River, Nevada, USA, which occurred between 1994 and 2019. Their study emphasized the significant influence of hydrographic stage, sinuosity and planform asymmetry of individual meanders in determining the timing and location of cutoff events. They found that upstream-skewed meanders were more prone to cutoff, potentially due to the increased impact of floodwater against the inner banks and necks of meanders during bankfull stages.

In a separate study, Wu *et al*. (2023) performed experiments that indicated medium and high discharge played a significant role in neck-cutoff, with cutoff events primarily occurring during periods of high discharge. While both studies provided valuable insights into the mechanisms of meander cutoff, neither study quantified the critical discharge or flow conditions at which cutoff occurs.

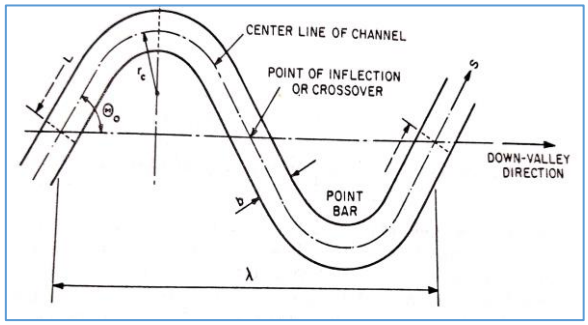

Fig. 1: Definition sketch of a river meander bend, after Odgaard (1986)

Although these studies contributed to our understanding of meander cutoff processes, the determination of the specific discharge or flow conditions at which cutoff events take place was not addressed. It will be presented herein the threshold values or criteria that can help quantify the critical discharge or flow conditions leading to meander-cutoff. Such quantification would provide valuable information for predicting and managing meander cutoff events which are a sort of different type of channel migration in river systems.

It is important to note that in order to describe the horizontal movement or migration of a point on a river centerline, its two-dimensional motion must be expressed using two coordinates, which require two equations. However, existing methods in the past have typically provided only one equation, which describes lateral bank erosion or migration. As a result, a complete two-dimensional description of the movement is not offered by these methods. In this study, we aim to address this limitation by providing two equations that fully define the movement of any point on the centerline of a meander bend.

For a point with two-dimensional polar coordinates (r, θ), we will provide an equation for the change in the radial coordinate (r) and another equation for the change in the arc angle (θ), thereby offering a complete description of the motion or migration in the two-dimensional horizontal plane. It is worth noting that θ represents the bend arc angle between the longitudinal (streamwise) and downvalley direction, which is also the angle between the radius of curvature line and the line perpendicular to the down-valley axis. Positive rotation is considered counter-clockwise for θ and vice versa.

In this study, we utilize regime equations, the extremal methods within the framework of the response theory proposed by Hafez (2000) and the excess-energy theory proposed by Hafez (2022). This combination facilitates the development of relations for predicting the dynamics of river channel migration. The purely theoretical and physically-based approach of this study offers the advantage of not requiring extensive data sets for model calibration, as seen in excess-bank velocity or excess-shear stress models. Additionally, the proposed approach considers all the influencing variables on river meander

DOI: 10.3844/ajessp.2025.12.38

migration and avoids the need to rely on sediment transport formulas, which often have uncertainties associated with their use.

The proposed purely theoretical and physically-based river migration model is based on two concepts: The minimum transverse energy loss slope (or minimum transverse power expenditure) and extremal channel sinuosity. These concepts provide two equations that are sufficient for a complete description of the movement of a point on the river centerline in two dimensions. The model offers several advantages:

1. It predicts both lateral meander growth and the reverse tendency of meander cutoff
2. It includes the effects of changes in various influencing variables on river migration, such as flow and sediment discharges, width, depth and roughness. This is different from most current models which focus on a single variable, such as excess velocity or excess shear stress
3. It does not rely on empirical coefficients found in current models, such as the bank erosion coefficient. Although it is a theoretical model, it has been validated by successfully predicting the meander wavelength in the Nile River, Egypt and the river channel radius of curvature in four USA Rivers
4. It accurately predicts the direction of river meander migration or the tendency for meander cutoff
5. It establishes a connection between changes in channel width and channel migration
6. It predicts the final equilibrium river channel planform, which occurs over long time scales, unlike current models that are primarily developed for small time scales
7. The model quantifies the concept of the tendency of river channels to minimize work in turning and considers extremal sinuosity, which could be a key aspect of river channel migration
8. It provides two equations for changes in radial distance and arc angle, thereby considering bend skewness and offering a complete description of motion in the two-dimensional horizontal plane
9. The developed equations are dimensionless, making them independent of scale issues
10. The model does not require channel width to be constant
11. It can incorporate sediment load and bed aggradation/degradation effects
12. It can also predict thalweg channel meandering

Materials and Methods

The total energy loss slope in curved meandering channel could be partitioned into two parts, the first is due to frictional resistance by the bed and banks (boundary friction) as in straight channels and the second is due to resistance caused by channel curvature in accordance with Chang (1992), i.e.:

$$S = S' + S'' \tag{20}$$

where, S is the total energy loss slope due to both of boundary friction and curvature, S' is the energy slope loss due to boundary friction by the bed and banks and S'' is the energy loss transverse slope due to curvature. Chang (1992) followed by Hafez (2000) have shown that straight river channel sections attain dynamic equilibrium by the tendency to minimize the longitudinal energy loss slope (S') and this condition is used as a closure equation to obtain an equation for determining the channel width. As both of S' and S'' are positive quantities by definition, the condition of minimum S implies that S' and S'' are minimum too. The assumption of a minimum transverse energy loss slope S'', is similar to the postulate by Leopold and Langbein (1966) that river channels meander while doing the least work in turning.

Equation (18) is easier to differentiate than Eq. (17) therefore it is combined with Eq. (16) as:

$$S'' = \left(12\,\frac{\sqrt{g}}{C} + 30\,\frac{g}{C^2}\right)\left(\frac{D}{r}\right)^2 F_r^2 \tag{21}$$

Assuming a wide and rectangular channel cross section, the square of the Froude number, F_r, in Eq. (21) could be written as:

$$F_r^2 = \frac{Q^2}{g\,B^2\,D^3} \tag{22}$$

Substituting Eq. (22) into Eq. (21) yields:

$$S'' = \left(12\,\frac{\sqrt{g}}{C} + 30\,\frac{g}{C^2}\right)\left(\frac{D}{r}\right)^2 \frac{Q^2}{gB^2\,D^3} = \Phi(C)\frac{1}{r^2}\frac{Q^2}{g\,B^2\,D} \tag{23}$$

Now, according to "the Response Theory" by Hafez (2000), for the condition of the transverse energy loss slope to be a minimum this implies that:

$$\frac{\Delta S''}{S''} = 0 \tag{24}$$

Applying Eq. (24) to Eq. (23) results in:

$$\frac{(\Phi(C))'}{\Phi(C)}\,\Delta C - 2\,\frac{\Delta r}{r} + 2\,\frac{\Delta Q}{Q} - 2\,\frac{\Delta B}{B} - \frac{\Delta D}{D} = 0 \tag{25}$$

where:

$$(\Phi(C))' = \frac{d\,(\Phi(C))}{dC} = \left(-12\,\frac{\sqrt{g}}{C^2} - 60\,\frac{g}{C^3}\right) \tag{26a}$$

Therefore;

$$\frac{(\Phi(C))'}{\Phi(C)} = -\frac{2}{C}\,\frac{\left(\sqrt{g}+5\frac{g}{C}\right)}{\left(2\sqrt{g}+5\frac{g}{C}\right)} \tag{26b}$$

And:

DOI: 10.3844/ajessp.2025.12.38

$$\frac{(\Phi(C))'}{\Phi(C)}\,\Delta C = -\frac{2\left(\sqrt{g}+5\frac{g}{C}\right)}{\left(2\sqrt{g}+5\frac{g}{C}\right)}\frac{\Delta C}{C} = -\Psi(c)\,\frac{\Delta C}{C} \tag{26c}$$

where:

$$\Psi(C) = \frac{2\left(\sqrt{g}+5\frac{g}{C}\right)}{\left(2\sqrt{g}+5\frac{g}{C}\right)} \tag{26d}$$

From the Chezy's equation for wide rectangular channels ($C = U/\sqrt{D\,S}$) the following equation can be obtained for ΔC/C:

$$\frac{\Delta C}{C} = \frac{\Delta U}{U} - \frac{1}{2}\frac{\Delta D}{D} - \frac{1}{2}\frac{\Delta S}{S} \tag{26e}$$

Now solving in Eq. (25) for the term containing the channel radius of curvature, *r*, yields:

$$\frac{\Delta r}{r} = \left\{-\frac{1}{2}\Psi(C)\,\frac{\Delta C}{C} + \frac{\Delta Q}{Q} - \frac{\Delta B}{B} - \frac{1}{2}\frac{\Delta D}{D}\right\} \tag{27}$$

Equation (27) gives the change in the channel radius of curvature on the left hand side of the equation due to changes in channel roughness, discharge, width and depth in the right hand side. Thus, Eq. (27) constitutes a meander migration model as it predicts the change in the channel radius of curvature due to changes in discharge, width, depth and roughness from flow regime to another flow regime, i.e., changes in regime over time. It should be noted that Eq. (27) is based on the assumption that the curved meandering river channel in its tendency toward dynamic equilibrium, it does so by minimizing the transverse energy loss slope which is analogous to doing the least work in turning. It is assumed for now that the meander bends are freely to move and migrate or in other words the banks are not restricting bank movements but bank resistivity will be considered and addressed later. The quantity $\Delta r = r_2 - r_1$ is the difference between the final channel radius of curvature and its initial value could be the radius of curvature after and before of a flood that caused lateral meander migration. The final value of *r* corresponds to final values of *C*, *Q*, *B* and *D*. The change in the variables could be for example due to the occurrence of a flood or a drought or the construction of a river structure such as a dam or change of the river reach from one regime to another regime due to roughness changes. Therefore, the incremental changes in the variables are understood to be variations with respect to time, i.e. time variations.

Several other forms similar to Eq. (27) could be obtained in terms of other variables as follows. The Froude number in Eq. (22) could be also expressed for a wide and rectangular cross section as $F = U/\sqrt{g\,D}$ and substituted in Eq. (21) to yield:

$$S'' = \Phi(C)\,\frac{D}{r^2}\,\frac{U^2}{g} \tag{28}$$

Applying Eq. (24) to Eq. (28) and solving for $\Delta r/r$ yields:

$$\frac{\Delta r}{r} = \left\{-\frac{1}{2}\,\Psi(c)\,\frac{\Delta C}{C} + \frac{\Delta U}{U} + \frac{1}{2}\,\frac{\Delta D}{D}\right\} \tag{29}$$

Equation (29) expresses the meander migration or bank displacement Δr in terms of change or excess in the velocity, flow depth and friction. It can be regarded as a purely theoretical generalization of the well-known bank erosion or meander migration equation, Eq. (1), by Ikeda *et al*. (1981) which adopts spatial difference in velocity while Eq. (29) adopts time difference. It takes time for any excess in velocity to cause meander migration, so Eq. (29) appears more natural in expressing meander migration.

Another equation could be developed by recognizing that the longitudinal boundary shear stress, τ, could be given for wide rectangular channels as: $\tau = \gamma\,D\,S$ where S is the longitudinal channel slope. When the shear stress is substituted via the channel depth, *D*, in Eq. (21) and application of Eq. (24) to the resulting equation, one obtains:

$$\frac{\Delta r}{r} = \left\{-\frac{1}{2}\,\Psi(C)\,\frac{\Delta C}{C} + \frac{\Delta U}{U} + \frac{1}{2}\,\frac{\Delta \tau}{\tau} - \frac{1}{2}\,\frac{\Delta S}{S}\right\} \tag{30}$$

Equation (30) includes both of the excess (incremental change) velocity and excess (incremental change) boundary shear stress and therefore could be considered as a generalization but in time of both the excess velocity and excess boundary shear migration models.

Alternatively, the quantity, transverse stream power or transverse power expenditure (P'') where $P'' = \gamma\,Q\,S''$ could be also assumed to attain a minimum value as a condition of dynamic equilibrium during the stream adjustment to the imposed flow and sediment conditions. In a similar fashion as before, applying $\Delta P''/P'' = 0$ results in:

$$\frac{\Delta r}{r} = \left\{-\frac{1}{2}\,\Psi(c)\,\frac{\Delta C}{C} + \frac{3}{2}\frac{\Delta Q}{Q} - \frac{\Delta B}{B} - \frac{1}{2}\,\frac{\Delta D}{D}\right\} \tag{31}$$

Equation (31) differs from Eq. (27) in the coefficient of the relative change in the discharge term ($\frac{\Delta Q}{Q}$) which is 1.5 in Eq. (31) instead of being 1.0 in Eq. (27).

Leopold and Wolman (1957) reports that the channel wave length, λ, is connected to the channel radius of curvature as:

$$\lambda \approx 4.7\,r \tag{32}$$

Regardless of the value of the constant in Eq. (32), or assuming: $\lambda \approx c\,r$, where c is any constant, it can be concluded that:

$$\frac{\Delta \lambda}{\lambda} = \frac{\Delta r}{r} \tag{33}$$

Equation (33) states that the relative changes (not the change itself) of the channel wave length and radius of

DOI: 10.3844/ajessp.2025.12.38

curvature are equal. This finding could be used to express the relative change in λ from Eq. (27) as:

$$\frac{\Delta\lambda}{\lambda} = \left\{-\frac{1}{2}\,\Psi(c)\,\frac{\Delta C}{C} + \frac{\Delta Q}{Q} - \frac{\Delta B}{B} - \frac{1}{2}\,\frac{\Delta D}{D}\right\} \quad (34)$$

Similarly Eq. (31) could be also used to find the relative change in λ assuming minimum transverse power expenditure, i.e.:

$$\frac{\Delta\lambda}{\lambda} = \left\{-\frac{1}{2}\,\Psi(c)\,\frac{\Delta C}{C} + \frac{3}{2}\frac{\Delta Q}{Q} - \frac{\Delta B}{B} - \frac{1}{2}\,\frac{\Delta D}{D}\right\} \quad (35)$$

Equations (34-35) will be used to test the proposed approach here because measuring of the meander channel wave length is easier from aerial maps and satellite images than measuring of the channel radius of curvature especially in the case of the field data of the Nile River, Egypt. Guo *et al*. (2019) had to use smoothing and filtering techniques to calculate reliable radius of curvature free of noise at the Bai River, China. In the results section both of Eq. (27) for *r* and Eq. (35) for λ will be shown to agree very well with measured field data.

To express time variation and dynamic river migration evolution with time, Eq. (27) can be written as:

$$\frac{\Delta r}{r} = k(t)\,\left\{-\frac{1}{2}\,\Psi(c)\,\frac{\Delta C}{C} + \frac{\Delta Q}{Q} - \frac{\Delta B}{B} - \frac{1}{2}\,\frac{\Delta D}{D}\right\} \quad (36)$$

where,

$$k(t) = \left\{1 - e^{-E_0\,(t - t_0)}\right\} \quad (37)$$

The function $k(t)$ in Eq. (36) is assumed as a time decay function as in Eq. (37), E_o is a bank erodibility coefficient as in Eq. (1), t_0 is the initial time at which bank movement has been started and t is the time under consideration. At time = t_0, Eq. (36) gives $\Delta r = 0$ which means that bank erosion and meander migration have not started yet, while at time approaching infinity ($t \rightarrow \infty$ or very large time value), Δr becomes the final equilibrium bank erosion displacement at which Eq. (36) becomes equivalent to Eq. (27) and bank change is at its maximum. The time function in Eq. (37) can be also used as a multiplier in the rest of the equations: Eqs. (29-31), Eqs. (34-35) to reflect the dynamic river channel migration evolution with time. The same time decay function could be also applied to Eq. (19) in the context of the excess energy theory.

To reflect spatial distribution of the bank displacement, for a single meander bend with arc length equal to *M*, the following distribution function $k(s)$, where s is the curvilinear coordinate along the river channel axis starting from the beginning of the bend, could be assumed as:

$$k(s) = \frac{s\,(\frac{M}{2} - s)}{\frac{M^2}{16}} \quad (38)$$

At $s = 0$ and $s = M/2$, $K(s)$ is zero which means that the start and middle points of the meander bend are assumed fixed in its location during the migration process. At $s = M/4$ (bend apex), $k(s) = 1$, which means that bank displacement and meander migration is at maximum at the bend apex. Calibration with spatial data could be useful also.

Applying both of the time decay function $k(t)$ and the spatial distribution function $k(s)$, to Eq. (27) yields the variation in time and space of a river migration dynamic model for bank movement as:

$$\frac{\Delta r}{r} = k(s)\,k(t)\,\left\{-\frac{1}{2}\,\Psi(c)\,\frac{\Delta C}{C} + \frac{\Delta Q}{Q} - \frac{\Delta B}{B} - \frac{1}{2}\,\frac{\Delta D}{D}\right\} \quad (39)$$

where, $k(t)$ is given by Eq. (37) while $k(s)$ is given by Eq. (38).

To account for bank resistivity to erosion and its limitation on lateral meander migration, a bank resistivity index, R, is used as follows:

$$\frac{\Delta r}{r} = (1 - R)k(s)\,k(t)\,\left\{-\frac{1}{2}\,\Psi(c)\,\Delta C + \frac{\Delta Q}{Q} - \frac{\Delta B}{B} - \frac{1}{2}\,\frac{\Delta D}{D}\right\} \quad (40)$$

where, for completely free meandering R is set to zero while for completely very resistive banks (e.g. very stiff clay banks or banks with riprap) R is set to 1.0. Field measurements of the strength of the bank material could be used to determine R.

The foregoing developed equations gave the change in the radial coordinate (r). Now attention is given to develop an equation that gives the change in the arc angle (θ), θ here is Θ_o in Fig. (1). The meander path or the centerline could be approximated by circular arcs for which the arc-length (L) which is for a quarter of a bend = L/4 from basic mathematics is given by:

$$\frac{L}{4} = r\,\theta \quad (41)$$

Applying the differential operator to Eq. (41) yields:

$$\frac{\Delta L}{L} = \frac{\Delta r}{r} + \frac{\Delta\theta}{\theta} \quad (42)$$

From which:

$$\frac{\Delta\theta}{\theta} = \frac{\Delta L}{L} - \frac{\Delta r}{r} \quad (43)$$

Hafez (2022) developed an equation for the meander bend arc length, L, (called there as M) which could be given here as:

$$\mathrm{L} = 50.73\ \mathrm{D}\ \mathrm{f}^{-0.45} \quad (44)$$

Applying the differential operator, as in Eqs. (5-44) yields the relative incremental change in L as:

$$\frac{\Delta L}{L} = \frac{\Delta D}{D} - 0.45\,\frac{\Delta f}{f} \quad (45)$$

Substituting Eq. (45) into Eq. (43) results in the relative change of the θ coordinate, as:

DOI: 10.3844/ajessp.2025.12.38

$$\frac{\Delta\theta}{\theta} = \frac{\Delta D}{D} - 0.45\,\frac{\Delta f}{f} - \frac{\Delta r}{r} \quad (46)$$

where, the term $\Delta r/r$ on the right-hand-side in Eq. (46) could be given from the previously developed equations such as Eqs. (27, 34, 35), or the most general form presented by Eq. (40). Now Eq. (40 and 46) which are linked together provide two independent equations that give the change in the radial distance *r* and the arc angle θ, respectively; thus giving complete determination of the motion of any point on the centreline of a meander bend with original coordinates (r, θ). This is not offered by any of the past methods to the best of the author's knowledge. If Δθ is negative it means θ is decreasing and the meander bend is migrating downstream and when Δθ is positive it means upstream migration. In this way meander bend skewness could be modelled. Equation (46) is based on the geometrical constraint between r and θ as offered by Eq. (41). However the approach will be later improved by including an additional extremal concept namely extremal channel sinuosity. Due to the much involved mathematics this is presented at the end of the discussion section.

In summary, the river plan form is represented by the river channel centreline and it could be given in terms of the polar coordinates (r, θ) at any time, t. Due to any changes in the influencing variables such as the flow discharge, channel width, channel depth, sediment load and roughness, the change or perturbation in r (i.e. Δr) and another perturbation in θ (i.e. Δθ) could be given according to the developed equations above such as Eq. (40 and 46). Thus the point (r, θ) will be (r + Δr, θ+Δθ) at a later time.

It should be noted that the radial distance r could be given in several ways. One way is to approximate the meander centreline into circular arcs, another is to use Eq. (19) for r, or lastly is to use the well-known equation of the sine-generated curve, Leopold and Langbein (1966), as follows:

$$\theta = \theta_o \cos\left(\frac{2\pi}{L} s\right) \quad (47)$$

where, θ_o is the initial deflection arc angle and s is the curvilinear coordinate along the channel axis. Leopold and Langbein (1966); Langbein and Leopold (1966); Da Silva (2006) report that a natural regular meander is best idealized by the sine-generated-curve. The radius of curvature could be given from Eq. (47) as:

$$\frac{1}{r} = \left|\frac{d\theta}{ds}\right| \quad (48)$$

Applying Eqs. (48-47) gives an equation for the radial coordinate *r* as:

$$r = \frac{1}{\frac{2\pi}{L}\theta_o \sin\left(\frac{2\pi}{L} s\right)} \quad (49)$$

Now a brief analysis on the formation of meander cutoff is given. Formation of cutoffs whether it is a neck or chute cutoff is an important part of river migration dynamic evolution. A trial is made here to estimate the critical discharge at which a meander bend goes into a neck-cutoff and also a chute cutoff. Due to different conditions of water and sediment and the composition of riverbank material, the occurrence modes and processes of neck cutoff also vary, (Hooke, 2004). According to the causes of cutoff, neck cutoff can be divided into three modes: Bank collapse mode, punching mode and string groove mode, (Hooke, 2004). In the bank collapse mode, the reason for cutoff is that the banks on both sides of a neck section collapse, or the bank on one side collapses. In punching mode, the floodplain current scours and forms new grooves. In string groove mode, the first flood scours the floodplain to form a series of gullies and subsequent floods continue to scour along the formed series of gullies and can mainly be traced to the source, (Hooke, 2004). Constantine *et al*. (2010) report that chute cutoff is initiated during a flood by the incision of an embayment.

Consider an existing meander bend assumed to go into a neck-cutoff process. It can be noted that neck-cutoffs occur when the initial meander or bend angle is greater than π/2, Fig. (2). To simplify the mathematics, the main river channel bend cross section is assumed rectangular in shape with a width of *B*, a depth of *D* and with a neck space (called neck width in the literature) of *x*. A high flood coming to the bend is assumed in the form of a horizontal water jet with discharge *Q*, average longitudinal velocity *U* and water density ρ. This jet would have a momentum force equal to $F = (\rho\ Q\ U)$ according to basic fluid mechanics laws. For this jet to cause a neck cutoff it has to erode the volume of material in the neck region which assumed to have a length of *x*, width of B_1 and depth of D_1 assuming for simplicity rectangular cross section. The neck-cutoff channel is assumed in general to have dimensions different from the upstream channel bend. The neck-region has material with a particle unit weight of γ_s and assumed saturated with water from previous floods. Effects of vegetation and other obstacles in the neck cutoff region could be considered via introducing momentum transfer efficiency factor η.

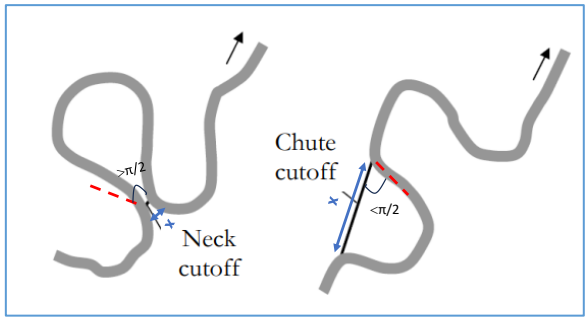

Fig. 2: Neck- and chute-cutoffs

DOI: 10.3844/ajessp.2025.12.38

In investigating bridge pier scour by Hafez (2016a); also in investigating scour due to horizontal turbulent wall jets downstream of barrages and low-head hydraulic structures by Hafez (2016b); and in investigating plunge pool scour by Hafez (2018); an energy balance theory was introduced for local scour which is helpful in modelling the scouring process caused by the cutoff processes. The energy balance theory states that the final equilibrium scour volume geometry is obtained through the balance of the work done by the attacking fluid flow jet and the work needed to remove the scoured material volume away or out of the scoured region. The energy balance theory is applied first to the neck-cutoff case herein as follows.

The flow jet would have to exert work equal to η. *F*. *x*/2 = η ρ *Q U x*/2. The work distance is *x*/2 because theoretically speaking the flow jet would move the upstream particles (the start of the neck-region) in the neck-region a distance *x* while it would move the downstream particles (at the end of the neck-region) a distance equal to one particle size which could be assumed practically as zero. Upon taking averaging of all the distances moved by all the particles the average distance would be *x*/2. From the laws of mechanics the work done by the group of forces is equal to the work done by the resultant of these forces. This gives another alternative to justification of the distance *x*/2 by considering moving out of the neck-region the center of mass of the neck volume which is located at *x*/2. The work done in moving out the particles in the neck-volume is the submerged weight of the neck-volume-material multiplied by the dynamic friction coefficient and then multiplied by the average distance of movement of *x*/2, i.e., equal to (γ_s- γ) B_1 D_1 *x* (tan ϕ) (*x*/2), where γ_s is the unit weight of the neck-volume-material, γ is the water unit weight, ϕ is the angle of repose of sediment and tan ϕ is the dynamic friction coefficient. Equating the work due to the attacking flow jet to the work required in moving the scoured volume out of the neck region and solving for the discharge *Q* (called Q_{cr-nk}, i.e., the critical discharge for incipient of meander neck cutoff) results in:

$$Q_{cr-nk} = \frac{(\gamma_s - \gamma)}{\eta\ \rho}\ \frac{B_1 D_1\ x}{U} = g\ (S_g\ - 1) \frac{B_1 D_1\ x \tan(\phi)}{\eta\ U} \qquad (50)$$

where, g is the gravitational acceleration and S_g is the sediment specific gravity (S_g = 2.65 for sand). With the velocity U= Q/(BD), Eq. (50) will be:

$$Q_{cr-nk} = \frac{(\gamma_s - \gamma)}{\eta\ \rho}\ \frac{B_1 D_1\ x}{U} = \sqrt{\frac{g}{\eta}\ (S_g\ - 1)\ B\ D\ B_1 D_1\ x\ \tan(\phi)} \qquad (51a)$$

Equation (51a) gives the critical discharge at which erosion of the neck-volume material would start and formation of a neck cutoff occurs. Equation (51a) could be simplified further by assuming rectangular neck cutoff channel cross section and that the cross section of the neck cutoff channel has width and depth equal to that of the original channel bend (i.e., B_1= *B* and D_1 = *D*) ; which simplifies Eq. (51a) to:

$$Q_{cr-nk} = B\ D \sqrt{\frac{g}{\eta}\ (S_g\ - 1)\ x\ \tan(\phi)} \qquad (51b)$$

As a numerical illustration, for a channel bend with width = 20 m, depth = 3 m, with tan ϕ ≈ 0.4, η ≈ 1 .0 and for a neck-distance of x = 30 m, Eq. (51b) gives a critical discharge of 836 ≈ 840 m^3/s at which meander cutoff would start. If there are vegetation or trees in the neck region by which η is assumed as 0.5, the critical discharge increases to about 1180 m^3/s. When tan ϕ is in the range of 0.4- 0.5, the meandering channel transverse bed slope equation by Bridge (1977) fits laboratory and natural point-bar profiles, so a value of tan ϕ ≈ 0.4 seems reasonable. However, it should be noted that ϕ depends on the size of the sediment particles and the degree of wetting which requires further investigations. According to Eq. (51a) if the new neck-cutoff channel has dimensions less than the original river bend dimensions then the critical discharge for cutoff occurrence would be less.

If the discharge is much higher than the critical value, the attacking jet would have more eroding force and more energy to move much more material than the material found in the neck-cutoff region. In that case the neck-cutoff distance will increase and could be given according to Eq. (51a) as:

$$x = \frac{\eta\ Q^2}{g\ (S_g - 1) \tan(\phi)\ B_1 D_1\ B\ D} \qquad (51c)$$

The discharge *Q* in Eq. (51c) is the flood discharge coming to the bend which is supposed to be much higher than the critical discharge for incipient of neck-cutoff. As an illustration, for a discharge of 2000 m^3/s (which is more than the critical discharge of 840 m^3/s) and with the same values for the other variables as in the last example, the length or distance of the newly formed neck cutoff would be about 171.6 m or ≈ 172 m which is about six times the neck-cutoff distance found before under critical discharge conditions of 840 m^3/s.

For chute cutoffs, it can be assumed that they occur when the initial bend angle is less than π/2, Fig. (2). Cases at the Sacramento River, Ca, USA, discussed in Constantine *et al.* (2010) show that chute cutoff approximately connects the two ends of the bend which means that the length of the chute cutoff could be assumed as the wavelength, λ, i.e., *x* ≈ λ as in Fig. (2). In this case the critical discharge for incipient chute cutoff (Q_{cr-ch}) could be given from Eq. (51a) by assuming x ≈ λ as:

$$Q_{cr-ch} = \sqrt{\frac{g}{\eta}\ (S_g\ - 1)\ B\ D\ B_1 D_1\ \lambda\ \tan(\phi)} \qquad (52)$$

Equation (52) could be used to investigate existing chute-cutoffs which could have a known length λ and known chute channel dimensions (assumed initially equal to that of the original bend) to estimate the chute-cutoff forming discharge Q_{cr-ch} from Eq. (52). The relation λ ≈

6B could be used in Eq. (52). Using the values from the previous example yields a chute cutoff discharge equal to 1672.4 ≈ 1672 m^3/s. Further research is needed to determine the threshold between the neck- and chute-cutoff and to determine the start and end points of the chute-cutoff channel. Field data could be used to calibrate Eq. (51 and 52) by introducing a coefficient which accounts for the effects of the simplifying theoretical assumptions made such as rectangular channel cross section, vegetation and the assumption that: tan ϕ is 0.4.

Results and Discussion

Results

This study examines two field cases where the developed equations from the present approach are compared with measured field data. These two cases are chosen due to existing of a complete data set as finding a complete data set is very challenging and often is rare. One case focuses on the Nile River in Egypt to estimate the meander wavelength, while the second case estimates the meander radius of curvature for four rivers in Texas, USA. The Nile River case is particularly interesting due to a significant change in meander wavelength caused by the construction of a major dam: the Aswan High dam. The advantage of this data is that it includes changes in flow discharge, channel width and channel depth, which are related to the variations in meander wavelength. Most meander migration studies typically report data on a single variable, such as velocity or shear stress. To address the lack of hydraulic and roughness data required for meandering investigations, Chang (1992); Hafez (2022) have emphasized the necessity of theoretical and analytical work preceding data collection efforts. This approach helps avoid limitations imposed by data characteristics that may hinder the study outcomes. Often, researchers collect data first and then attempt to identify relationships among the variables. However, this practice limits the study outcomes to the type, quality and volume of available data.

The Nile River in Egypt spans a distance of approximately 1160 km and is divided into four reaches between Aswan in the south to Cairo in the North by existing dams and barrages, as shown in Fig. (3) (NRI, 1992). The construction of the Aswan High Dam (AHD) in 1968 led to significant changes in the flow characteristics downstream of the dam, including a considerable reduction in flow discharge and sediment load due to dam storage of sediment. For example, the mean monthly maximum discharge downstream of AHD decreased from 8400 m^3/s in the pre-AHD conditions to 2560 m^3/s in the post-AHD conditions. This dramatic change in peak flows and subsequent alterations in river regime had substantial effects on the planform geometry of the Nile, particularly the meandering pattern as shown in Tables (1-2). Before the construction of AHD, during flood seasons, all barrage gates were open to allow high flood flows, which maintained a relatively constant river regime over the years, resembling a natural state. After AHD, the barrage gates were partially opened to accommodate only the discharge required for agricultural, domestic and industrial needs, which was significantly lower than pre-AHD conditions.

The thalweg meander wavelengths, as defined in Fig. (4), were measured from hydrographic maps dating back to 1982 for six approximately 20 km reaches (Table 1). Reaches with well-defined meander patterns, as depicted in Fig. (5), were selected for analysis where it can be seen the near equality of the river channel and thalweg meandering. Moving downstream, Table (1), the thalweg wavelength decreased from a maximum of 4500 m upstream of Isna Barrage to a minimum of 2500 m downstream of Asyut Barrage. However, it then increased to 3300 m upstream of Delta Barrages near Cairo. The decrease and subsequent increase in thalweg wavelength in the downstream direction align with the changes in peak discharge, which also decrease and then increase (NRI, 1992).

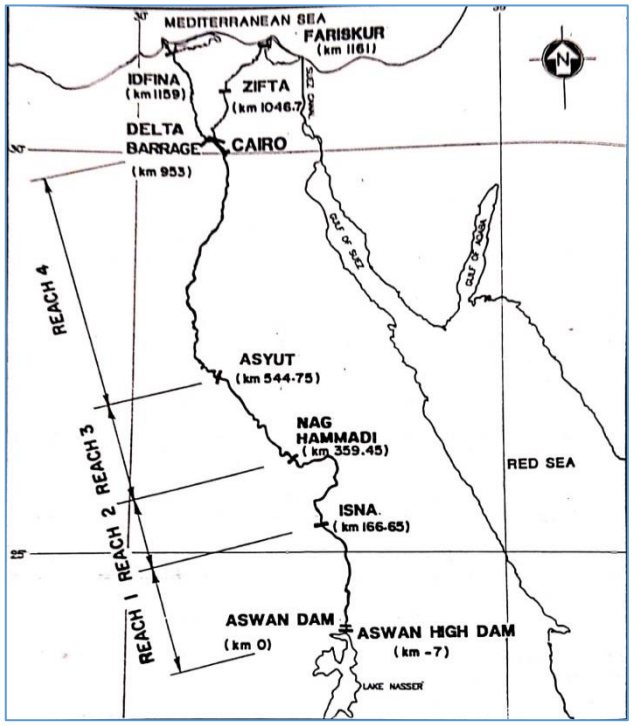

Fig. 3: Schematic layout of the Nile River, Egypt with existing hydraulic structures of dams and barrages, after NRI (1992)

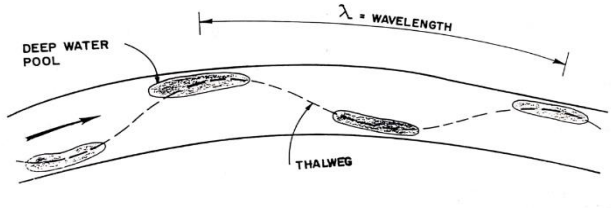

Fig. 4: Definition of thalweg meander, after NRI (1992)

DOI: 10.3844/ajessp.2025.12.38

Table 1: Approximate 1982 thalweg meander wavelength

Reach Name	Reach classification	Reach location (km)	Thalweg meander wavelength (m)
Idfu	First reach	110-130	4500
Shanhoria	Second reach	244-264	4000
Girga	Third reach	398-420	3000
Hawata	Fourth reach	596-620	2500
Beni Mazar	Fourth reach	727-750	2700
Geziret el Makatfiya	Fourth reach	856-876	3300

Table 2: Measured regime characteristics of the Nile River, Egypt (Pre-AHD), NRI (1992)

Reach Number	Mean monthly maximum discharge (m^3/s)	Channel width (m)	Channel depth (m)	Meander wavelength (m)
1	8400	878	9.96	5268
2	8180	794	11.12	4764
3	7640	924	11.2	5544
4	7460	1025	9	6150

In this study, the meandering thalweg line is chosen instead of the channel centerline, in contrary to previous studies. This decision is motivated by the fact that in natural meandering rivers, defining the channel centerline at midpoints across the channel width can result in irregular lines due to variations in spatial channel widths and the presence of islands and bars. Defining the thalweg line, which represents the deepest points along the river course (as shown in Fig. 4), is more convenient as it corresponds to the flow path and represents a unique case of flow curvature considered in this study.

Due to the lack of pre-Aswan High Dam (AHD) hydrographic mapping the thalweg wavelength for that period is unknown (NRI, 1992). However, it can be estimated using the relationship $\lambda = 6B$ (Eq. 14), as shown in Table (2), which also includes the discharge, width and depth for each reach under pre-AHD conditions. Table (3) presents the same data but for the post-AHD conditions. Note that in Table (3), the thalweg meander wavelength in the three sub-reaches located in the fourth reach is averaged.

The success of the relation $\lambda = 6B$ (Eq. 14) in predicting the post-AHD thalweg wavelength, with a predicted/measured ratio ranging from 0.85 to 1.18, supports its use in estimating the pre-AHD thalweg wavelength.

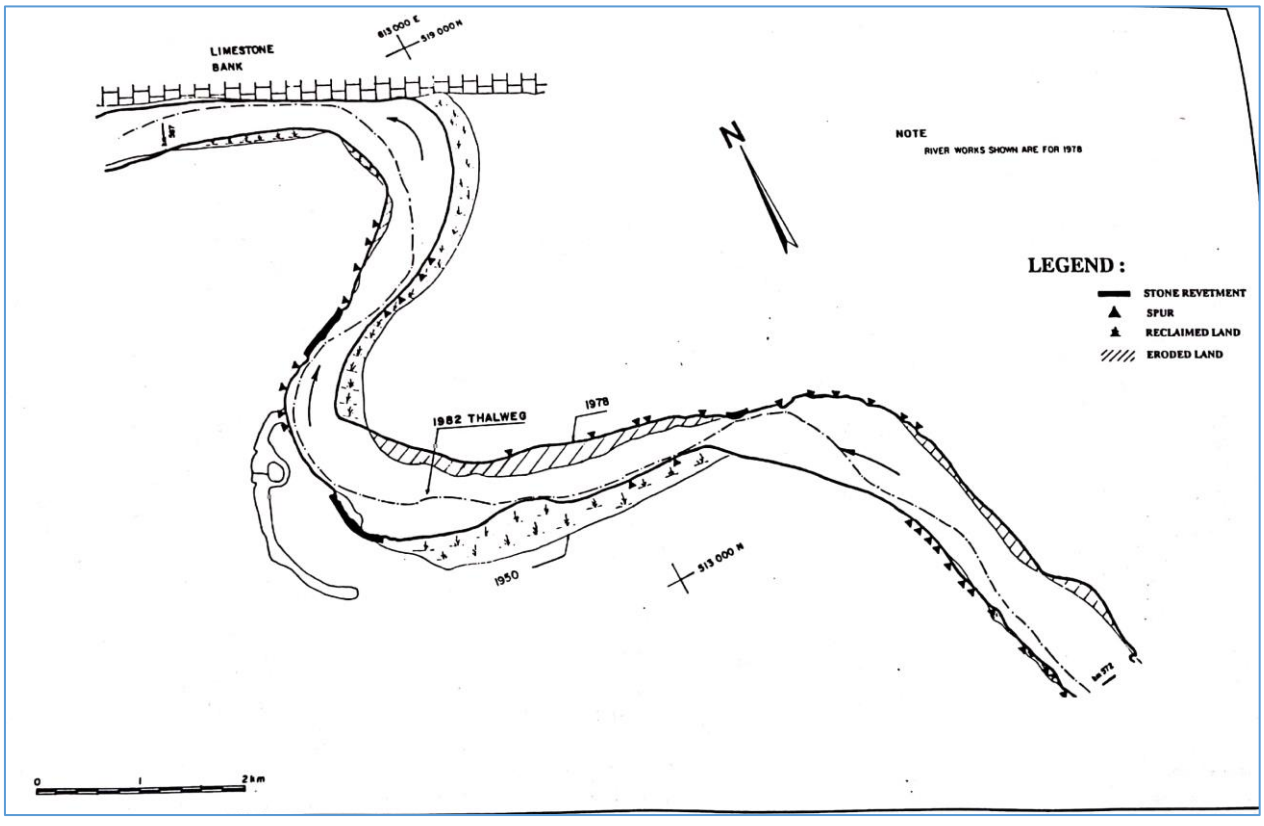

Fig. 5: Nile River in Egypt thalweg and river channel meander, after NRI (1992)

DOI: 10.3844/ajessp.2025.12.38

Table 3: Measured regime characteristics of the Nile River, Egypt (Post-AHD), NRI (1992)

Reach Number	Mean monthly maximum discharge (m^3/s)	Channel width (m)	Channel depth (m)	Measured Meander wavelength (m)	Calculated Meander wavelength (m)	Ratio of calculated to measured wave length
1	2560	634	6.83	4500	3804	0.85
2	2350	569	5.7	4000	3414	0.85
3	2110	588	5.9	3000	3528	1.18
4	1690	538	4.89	2830	3228	1.14

The calculation of the thalweg meander wavelength for the post-AHD condition of the first reach is provided in detail and a similar procedure can be followed for the other three reaches. The relative changes in discharge, width and depth are calculated as follows, with subscripts 1 and 2 denoting the pre- and post-AHD conditions, respectively:

$$\frac{\Delta Q}{Q} = \frac{Q_2 - Q_1}{Q_1} = \frac{2560-8400}{8400} = -0.695 \quad (53)$$

$$\frac{\Delta B}{B} = \frac{B_2 - B_1}{B_1} = \frac{634-878}{878} = -0.278 \quad (54)$$

$$\frac{\Delta D}{D} = \frac{D_2 - D_1}{D_1} = \frac{6.83-9.96}{9.96} = -0.314 \quad (55)$$

To use Eq. (34) and find the post-AHD thalweg wavelength, which will be compared against measured values, information is required about the first term on the right side involving the relative change in roughness in terms of Chezy's coefficient. It was found by NRI (1992) that the water surface slopes are nearly the same for the pre- and post-AHD conditions. For example, reach 1 has pre- and post-AHD measured slopes of 0.05 m/km. As the differences are nill, it can be assumed that roughness changes are negligible for the computations. Substituting the values obtained from Eq. (53-55) into Eq. 34 yields:

$$\frac{\Delta\lambda}{\lambda} = \{0 - 0.695 - (-0.278) - 0.5\,(-0.314)\} = -0.26 \quad (56)$$

For a value of λ_1, according to Table (2) for the first reach, of 5268 m, the predicted post-AHD thalweg wavelength is:

$$\lambda_2 = \left(1.0 + \frac{\Delta\lambda}{\lambda}\right)\lambda_1 = (1.0 - 0.26)\,(5268) = 3898 \approx 3900\,m \quad (57)$$

It is worth noting that $\Delta\lambda/\lambda = \Delta(\lambda/2)/(\lambda/2)$, so the equations remain valid whether the thalweg wavelength, as shown in Fig. (3), appears to be half of the typically defined channel wavelength. The computed value of 3900 m obtained from Eq. (57) is compared to a measured value of 4500 m, resulting in a relative error of approximately -13%. The ratio of the computed to measured thalweg wavelength is 0.87, while Eq. (14) also yields a close ratio of 0.85. Table (4) presents the thalweg wavelength computations for all the reaches using Eq. (34) and Eq. (35). Table (5) shows that Eq. (34) performs better in reaches number 1 and 2 while Eq. (35) preforms better in reaches number 3 and 4. Such situation is addressed in the discussion section.

The second case involves four rivers in Texas, USA: The Brazos River, the Nueces River, the Trinity River and the Guadalupe River (Briaud *et al*., 2001). Table (6) illustrates the significant changes that occurred in the channel width and radius of curvature of these rivers. Although the discharge data were presented graphically in terms of mean monthly discharges, it is well-known that river morphology changes are primarily associated with high flood flows, for which maximum flow data were not provided. Hence, we will rely on the regime theory relationship between discharge and width to address this limitation. In this case, width is considered a proxy for discharge and channel size, as discharge data are lacking. The width-discharge exponent, b, in Eq. (12) is assumed to be 0.5, based on studies by Lacey (1930; 1958); Blench (1952; 1970); Simons and Albertson (1960). Consequently, we assume:

$$\frac{\Delta B}{B} = b\,\frac{\Delta Q}{Q} = 0.5\,\frac{\Delta Q}{Q} \quad (58)$$

From Eq. (58), we can conclude that:

$$\frac{\Delta Q}{Q} = 2\frac{\Delta B}{B} \quad (59)$$

Since no information was provided about the depth and the slope remains constant in all cases, both the depth and roughness terms in Eq. (31) are neglected, assuming that their contributions cancel each other out. Substituting Eq. (58) into Eq. (31) yields:

$$\frac{\Delta r}{r} = \left\{\frac{3}{2}\left(2\,\frac{\Delta B}{B}\right) - \frac{\Delta B}{B}\right\} = 2\,\frac{\Delta B}{B} \quad (60)$$

We will first address the cases where the radius of curvature is directly proportional to the river channel width, as shown in Table (7). The remaining cases will be analyzed separately, as they require distinct treatment or analysis. For illustrative purposes, we will present the detailed example of meander change in the Brazos River at SH 105 (Case 1) between the years 1910 and 1958. The relative change in channel width during this period can be calculated using the data from Table (6):

$$\frac{\Delta B}{B} = \frac{B_2 - B_1}{B_1} = \frac{B_{1958} - B_{1910}}{B_{1910}} = \frac{98-109}{109} = -0.101 \quad (61)$$

Applying Eq. (60) gives a predicted $\Delta r/r$ = -0.202. Therefore, $\Delta r = (\Delta r/r) * r_1$ = (-0.202) * 747 ≈ -150.89 m, which is approximately -151 m. The measured Δr is 600-747 = -147 m. The predicted radius of curvature in 1958 is calculated as $r_2 = r_1 + \Delta r$ = 747-150.89 ≈ 596 m, while the measured radius in 1958 is 600 m, resulting in a very small relative error of about -0.7%. Unfortunately, the channel depth and friction data were not reported, which prevents the application of Eq. (46) to determine the change in the arc angle θ. The results of predicting six additional cases are presented in Table (7).

DOI: 10.3844/ajessp.2025.12.38

Table 4: Computation of thalweg meander wavelength of the Nile River, Egypt for the 1982 Post Aswan High Dam conditions

Reach	ΔQ/Q	ΔB/B	ΔD/D	Δλ/λ From Eq. (33)	Estimated pre-AHD λ_1 (m)	Computed λ_2 (m) according to Eq. (34)	Computed λ_2 (m) according to Eq. (35)	1982 Measured λ_2 (m)
1	-0.695	-0.278	-0.314	-0.260	5268	3900	2068	4500
2	-0.713	-0.283	-0.487	-0.187	4764	3875	3337	4000
3	-0.724	-0.364	-0.473	-0.124	5544	4856	2852	3000
4	-0.774	-0.475	-0.389	-0.106	6150	5498	3131	2830

Table 5: The thalweg meander-wavelength of the post-AHD, the Nile River, Egypt. E1: Ratio of calculated by Eq. (14) to measured wave length

Reach Number	Measured λ (m)	Calculated λ Eq. (14) (m)	E1*	Computed λ Eq. (34) (m)	E2**	Computed λ Eq. (35) (m)	E3***
1	4500	3804	0.85	3900	0.87	2068	0.46
2	4000	3414	0.85	3875	0.97	3337	0.83
3	3000	3528	1.18	4856	1.62	2852	0.95
4	2830	3228	1.14	5498	1.94	3131	1.11

E2**: Ratio of calculated by Eq. (33) to measured wave length; E3***: Ratio of calculated by Eq. (34) to measured wave length

Table 6: Summary of Case History Data for the four USA Rivers, Texas, Briaud *et al*. (2001)

Case History	Year	Channel width, B, (m)	Radius of curvature, r, (m)	Free surface slope (m/m)
Brazos	1910	109	747	0.00018
At SH 105	1958	98	600	0.00018
(case 1)	1981	84	453	0.00018
	1988	89	558	0.00018
	1995	133	460	0.00018
Brazos	1910	107	1733	0.00018
At SH 105	1958	107	1173	0.00018
(case 2)	1981	120	746	0.00018
Nueces	1958	134	365	0.0009
At US 90	1969	122	300	0.0009
(case 3)	1995	70	391	0.0009
Trinity	1971	125	182	0.00008
At FM 787	1976	73	182	0.00008
(case 4)	1983	112	??	0.00008
	1988	132	201	0.00008
	1999	155	276	0.00008
Guadalupe	1959	50	88	0.00037
At US 59	1981	58	88	0.00037
(case 5)	1988	54	100	0.00037
	1995	92	125	0.00037
Guadalupe	1959	42	137	0.00037
At US 59	1981	33	125	0.00037
(case 6)	1988	67	108	0.00037
	1995	75	104	0.00037

Table 7: Equation (60) Prediction of the radius of curvature at four USA Rivers in Texas

Case History	Period	Measured ΔB/B	Calculated Δr/r	Measured r at end of period (m)	Eq. (60) Predicted r at end of the period (m)	Briaud et al. (2001) Predicted r at end of the period (m)
Brazos At SH 105 (case 1)	1910-1958 1958-1981 1981-1988	- 0.101 - 0.143 + 0.060	- 0.202 - 0.286 + 0.120	600 453 558	596 429 507	- 530 408
Nueces At US 90 (case 3)	1958-1969	- 0.090	- 0.180	300	299	-
Trinity At FM 787 (case 4)	1971-1988 1971- 1999	+ 0.056 + 0.240	+ 0.112 + 0.480	201 276	202 269	- -
Guadalupe At US 59 (case 5)	1959-1988	+ 0.080	+ 0.160	100	102	88

DOI: 10.3844/ajessp.2025.12.38

Now special treatment is given to the rest of the special cases in Table (6). In these treatments some assumptions had been made in a way to match the observed data in as much as possible which could be considered as a sort of calibration process. This will aid in understanding river migration dynamic behaviour.

For the years 1988-1995 at Brazos River at SH 105 (Case 1), Table (6) shows that while the width increased from 89 to133 m the radius of curvature decreased from 558 to 460 m., i.e., large increase in width of 44 m with a large decrease in the radius of curvature of 98 m. The term $\Delta B/B$ = (133-89)/89 = 0.494. If it is assumed that width is proportional to discharge to a power of 3/2 this leads to $\Delta B/B = 3/2\ \Delta Q/Q$ from which $\Delta Q/Q = 2/3\ \Delta B/B$. Substituting this relation into Eq. (27) for the case of minimum transverse energy loss slope yields:

$$\frac{\Delta r}{r} = \frac{\Delta Q}{Q} - \frac{\Delta B}{B} = \frac{2}{3}\frac{\Delta B}{B} - \frac{\Delta B}{B} = \frac{-1}{3}\frac{\Delta B}{B} \quad (62)$$

Substituting the value of $\Delta B/B$ = 0.494 into Eq. (62) yields $\Delta r/r$ = - 0.165 and with r_1 = 558 m, this results in $\Delta r = (\Delta r/r) * r_1 \approx$ - 92 m and the predicted 1995 radius ($r_2 = r_1 + \Delta r$) becomes 466 m while the measured value is 460 m while Briaud *et al*. (2001) predicted a value of 663 m using the map sequence method.

At the second bend at Brazos River at SH 105 (Case 2) from 1910 to 1958, channel width did not change while dramatic decrease in the radius of curvature occurred from 1733 to 1173 m, i.e., with a decrease of -560 m. From the monthly discharge data it is noted the 1958 had flow of 1500 m^3/s but unfortunately there was no data records for the 1910 flows. A question arises: Could the historic river channel forming discharge in 1910 be estimated based on the morphological data changes in the radius of curvature? The measured $\Delta r/r$ = (1173-1733)/1733 = - 0.32. Adopting Eq. (27), with $\Delta B = 0$, neglecting ΔD and ΔC results in that $\Delta Q/Q = (2/3)\ \Delta r/r$ = - 0.213. Therefore $Q_1 = (1+\Delta Q/Q)\ Q_2$ = (1- 0.213) * 1500 ≈ 1906 m^3/s. Based on the given graphical data, three high flows of 1700 m^3/s in 1920, 1500 m^3/s in 1958 and 1400 m^3/s in 1990 appear to be the dominant maximum flows in this period. As discharge is proportional to the radius of curvature and since the maximum radius of curvature reported to be in the year 1910 it is expected that the year 1910 flow to be higher than 1700 m^3/s which occurred in 1920. If the minimum transverse energy loss slope is assumed, i.e. $\Delta Q/Q = \Delta r/r$, the 1910 flow would be about 2205 m^3/s. This case could be useful in determining historic flows based on changes in channel morphology.

The case at Brazos River at SH 105 (Case 2) from 1958 to 1981 is unique. The channel width in this period (23 years) increased from 107 to 120 m (about 12% increase) whereas the radius of curvature decreased dramatically by 426 m from 1173 to 746 m (36% decrease). The relative change in width $\Delta B/B$ = 0.121 according to the 1958 and 1981 widths and as such change is not significant in spite of the very large change in radius of curvature it can be assumed that the banks are relatively cohesive. The 1958 flow is 1500 m^3/s while the 1981 is about 600 m^3/s, so $\Delta Q/Q$ = - 0.6. The depth and velocity hydraulic regime exponents are taken according to Williams (1978) as f = 0.53 and m = 0.37 which represents conditions of cohesive but not vertical banks. The slope variation with discharge exponent can be taken according to Leopold and Maddock (1953) as 0.8 (this value for downstream hydraulic geometry is assumed valid herein). Substituting these values in Eq. (26d) gives $\Delta C/C$= 0.505 $\Delta Q/Q$. As it was found in the period from 1910 to 1958 that the minimum transverse energy loss slope is valid, this assumption will be also assumed to hold from 1958 to 1981. The Chezy's roughness coefficient could be assumed for rough bed conditions to have a value of C = 30, this value will make the left term of Eq. (26d) as:

$$\frac{(\Phi(C))'}{\Phi(C)}\Delta C = (-1.2) * \Delta C/C = (-1.2)\ (0.505)\ \Delta Q/Q = (-0.606)\ \Delta Q/Q \quad (63)$$

Equation (27) while substituting with the above values becomes:

$$\frac{\Delta r}{r} = \left\{-0.6 - 0.121 - \frac{1}{2}(0.53)(-0.6) + \frac{1}{2}(-0.606)(-0.6)\right\} = -0.38 \quad (64)$$

With 1958 radius of curvature r_1 = 1173 m and using Eq. (64) yields the predicted the 1981 radius of curvature equal to about 727.3 m versus a measured value of 746 m, with a relative error of about 2.5% while Briaud *et al*. (2001) predicted a 1981 radius of 905 m.

The case at Nueces River at US 90 (Case 3) had the width decreased from 122 m in 1969 to 70 m in 1995, while the radius of curvature increased from 300 m in 1969 to 391 m in 1995. Thus the term $\Delta B/B$ = (70-122)/122 = - 0.42. The flow discharges at the two years are practically zero however other flows must have formed the planform geometry. Before 1969, three high flows of 70, 100 and 90 m^3/s in 1954, 1958, 1965, respectively, with an average of 86.6 m^3/s and before 1995 another three high flows of 105, 95 and 75 m^3/s in 1972, 1974 and 1982 respectively with an average 91.7 m^3/s. If we consider the averages of these high flows then $\Delta Q/Q$ = (86.6-91.7)/91.7 = - 0.055. Substituting these values in Eq. (31) yields:

$$\frac{\Delta r}{r} = \left\{\frac{3}{2}\frac{\Delta Q}{Q} - \frac{\Delta B}{B}\right\} = \{1.5 * (-0.055) - (-0.42)\} = 0.338 \quad (65)$$

With 1969 radius of 300 m and using Eq. (65), the 1995 radius becomes ≈ 401m while the measured one is 391 m with relative error of about 2.6%. Briaud *et al*. (2001) predicted a 1995 width of 146 m which is very low.

Table 8: Prediction of the radius of curvature at four USA Rivers in Texas

Case History	Period	Measured ΔB/B	Calculated Δr/r	Measured r at end of period (m)	Briaud *et al*. (2001) Predicted r at end of period (m)	Predicted r at end of period (m)	Assumptions
Brazos At SH 105 (case 1)	1988-1995	0.494	-0.165	460	663	466	b =1.5, Minimum S′′
Brazos At SH 105 (case 2)	1958-1981	0.121	-0.38	747	905	727.3	f= 0.53, m =0.37, $S \propto Q^{-0.8}$ C =30 Minimum S′′
Nueces At US 90 (case 3)	1969-1995	-0.42	0.338	391	146	401	Minimum γ Q S′′
Guadalupe At US 59 (case 5)	1988-1995	+ 0.704	+ 0.235	125	88	123.5	b = 0.75, Minimum S′′
Guadalupe At US 59 (case 6)	1959-1981	-0.210	-0.105	125		122.6	b =1.0, Minimum γ Q S′′
Guadalupe At US 59 (case 6)	1981-1988	1.03	-0.142	108	121	107.3	b =1.16, Minimum S′′
Guadalupe At US 59 (case 6)	1988-1995	0.119	-0.04	104	91	103.7	b =1.5, Minimum S′′

The last four special cases at the Guadalope River have a width exponent (b) different from 0.5 as seen in Table (8) and three of them adopt the minimum transverse energy loss slope. Although Briaud *et al*. (2001) use two field data sets in the calibration process while the present approach uses only one field data set, it can be seen from Table (8) the present approach predictions are much better than those by Briaud *et al*. (2001).

Discussion

It should be noted that the present approach developed equations such as Eq. (27) does not require initial perturbation or initial flow curvature of an initial straight channel to initiate meander migration. All is required are changes in the flow discharge, width, depth and roughness at which the river migrate or meander in order to minimize the transverse energy loss slope or minimize the transverse stream power. It is understood that the channel is initially at equilibrium regime which is disturbed due to changes in the flow discharge, sediment load, depth, width and roughness. Sediment load changes affect the longitudinal channel energy slope which in turn affects roughness, therefore roughness changes are indirect effect to changes in sediment and of course water flow changes. Past methods offer only one equation such as Eq. (1) or condition for determining bank movement, i.e. they provide one degree of freedom which cannot describe completely movement of a point in two-dimensional horizontal plane. The proposed approach provides two equations or two degrees of freedom as can be seen from Eqs. (40 and 46) by which complete description of movement of a point in two-dimensional horizontal plane is possible.

It is noted from Table (4) at the Nile River that the absolute value of the relative change in $\Delta Q/Q$ and $\Delta B/B$ increase going in the downstream direction, while that for $\Delta D/D$ increases but then decreases. The overall effect of these variations is that the absolute values of $\Delta\lambda/\lambda$ decrease down the river course. Because the pre-AHD wavelengths are not following the post-AHD wavelengths trend of decrease then increase the predicted wavelengths by Eqs. (34 and 35) could not follow that trend. Equation (34) predictions agree well with the measurements for the first and second reaches while Eq. (35) predictions agree well for the second, third and fourth reaches.

It is noted from Table (5) that at the first reach Eq. (34) gives the best predictions with measured to calculated wavelength of 0.87 followed by Eq. (14) with a very close ratio of 0.85 while Eq. (35) highly gives a very low ratio of 0.46. At the second reach, Eq. (34) gives the best ratio of 0.97 while Eq. (14) and Eq. (35) performs also well with ratios of 0.85 and 0.83, respectively. At the third reach Eq. (35) ratio of 0.95 is the best followed by ratio of 1.18 by Eq. (14) while Eq. (34) has a very high ratio of 1.62. For the fourth reach Eq. (34) continues to give a high ratio of 1.94 (i.e., computed value is almost as twice as measured value) while Eq. (35) and Eq. (14) have a very close ratios of 1.11 and 1.14, respectively. Thus the first and second reaches thalweg meandering wavelengths are best predicted by Eq. (34) which is based on the minimum transverse energy slope.

It can be stated that the wave lengths in the second, third and fourth reaches are well predicted by Eq. (35) which is based on the minimum transverse stream power. Several factors can be attributed to the discrepancy between the computed and measured wavelengths among which are data accuracy and the theoretical assumptions.

DOI: 10.3844/ajessp.2025.12.38

For example, the mean maximum monthly discharge data which was reported in NRI (1992) might be different from the meandering channel forming discharge. The negligence of the roughness term might be another factor and some doubt exists about the NRI (1992) reporting that roughness remains essentially indifferent before and after the construction of AHD dam. Also flows in the third and fourth reaches are increasing in the downstream direction. The pre-AHD estimated wavelengths based on Eq. (14) might be also a reason for the discrepancies. In addition, another factor is that the river has insufficient room to form a natural meandering pattern within the geomorphic confines of the overall channel, NRI (1992). As the river reaches are subjected to different hydraulic, hydrological and geologic conditions, every reach might be experiencing different extremal concept. It was shown using natural river field data that different extremal hypotheses or concepts are applicable to different rivers and sometimes two concepts or more are applicable to the same river reach, Hafez (2000; 2001a-b; 2002). This has to do with the size of the stream which could be expressed in terms of the stream longitudinal stream power, γQS. This distinction is left for future research.

Thus, it can be stated that the first and second reaches experience minimum transverse energy slope loss while the third and fourth reaches experience minimum transverse energy stream power. Of course, Eq. (14) is based on field data so it could be considered as a data in itself as well. Da Silva (2006) reports Eq. (14) is based on a very large number of field and laboratory measurements carried out mostly by Japanese researchers (Hayashi (1971; Task Committee on The Bed Configura, 1973). Even discrepancy among the data exist in the literature as Richards (1982) suggests that λ = (12.34) B. The Regime equation by Dury (1964), Eq. (13) did not perform well where the ratio of computed to measured wavelengths went as low as 0.61 and 0.66 at the first and second reaches, respectively. In spite of the challenge of data accuracy in this case, the results are very satisfactory.

It was shown that Eq. (29) could be a more general form of the classical bank erosion model based on excess velocity while Eq. (30) could also be a generalization but in time of the classical bank erosion model based on excess shear stress. Equations such as Eqs. (27, 29-30) are all dimensionless and in the form of a linear perturbation resulting from applying some extremal concept to an energy-related equation which represents river regime in balance. The well-known classical Ikeda *et al*. (1981) bank erosion model is considered a seminal work in the area of river dynamic migration resulting from a linear perturbation of the flow hydrodynamics and sediment governing equations. There are some analogies between Ikeda *et al*. (1981) approach and the present approach. This can be understood by comparing to numerical methods where the finite difference method approximates the governing differential equation while the finite element approximates the solution to the governing differential equation. The present approach approximates the solution which represents river regime dynamics in meandering rivers and as such is similar to the Finite Element method while Ikeda *et al*. (1981) approximates the governing equations whose solution represents river migration dynamics and as such is similar to the Finite Difference method.

The connection between the excess energy theory, Hafez (2022) and the present approach could be explained as follows. The excess energy theory derived equation, Eq. (15), has been shown to explain the causes of river curvature and meandering. Thus the quantity representing the transverse energy slope: $S'' = (S_V - S_R)$ explains the causes of river meandering while its minimization (i.e., $S'' = (S_V - S_R) \rightarrow minimum$), explains river meandering migration dynamics. Thus S'' explains meander initiation while the minimization of S'' explains meander migration dynamics or equivalently $(S_V - S_R)$ explains meander initiation while minimization of $(S_V - S_R)$ explains meander evolution and dynamics with time.

Inspection of Eqs. (27 and 31) reveals several important qualitative and quantitative observations. But first, it should be noted that the quantity Δr when it is increasing (Δr is positive, i.e., +) that means that the river reach radius of curvature increases and is going toward channel straightening or ultimately toward meander cut-off. Conversely, if Δr is negative or is decreasing that means that the channel reach radius of curvature is decreasing and curvature or the degree of meandering is increasing. To facilitate the matter further, Eq. (26d) is substituted into Eq. (27) resulting in:

$$\frac{\Delta r}{r} = \left\{ - \frac{\left(\sqrt{g} + 5\frac{g}{C}\right)}{\left(2\sqrt{g} + 5\frac{g}{C}\right)} \frac{\Delta C}{C} + \frac{\Delta Q}{Q} - \frac{\Delta B}{B} - \frac{1}{2}\frac{\Delta D}{D} \right\} \tag{66}$$

Assuming hypothetically that the channel width, depth and roughness are constants, while the discharge is the only varying and controlling variable. In this case Eq. (66) indicates that Δr is directly proportional to ΔQ. This means that when Q increases (ΔQ is +); Δr is + and consequently r is increasing, i.e., going into channel straightening or ultimately into meander cut-off. This means that the migrating river channel is absorbing the energy caused by increased discharge by increasing channel slope while keeping the same channel cross sectional dimensions. The opposite is true as reduction of Q leads to decrease in Δr and consequently increase in channel sinuosity and meandering degree which occur downstream of dams due to reduced flows as in the Nile River case. If the channel width (B) is the only variable such as when channel widening occurs due to bank erosion, then Δr is inversely proportional to ΔB, i.e., when ΔB is increasing Δr is decreasing and vice versa. Ferreira Da Silva and Ibrahimi (2017) stated that alluvial meandering streams are usually

DOI: 10.3844/ajessp.2025.12.38

rather wide objects (≈ 10 < B/D < ≈ 120). When depth is the only variable (such as through dredging processes) Δr is inversely proportional to ΔD, which indicates increase in channel depth (channel deepening) leads to more sinuous and meandering conditions while going into shallow depths lead to straightening conditions. It should be noted that roughness is inversely proportional to the Chezy's coefficient *C*, for example *C* = 60 is at smooth beds while *C* = 30 is at rough beds, Rozovskii (1957). Thus when roughness increases ΔC is negative and when roughness decreases ΔC is positive. Therefore, Δr is directly proportional to channel roughness and inversely proportional to the value of Chezy's *C*. This means that an increase in channel roughness would lead to channel straightening while a decrease in roughness increases the degree of curvature and meandering. All of these observations about the direction of change are in line with field observations by past investigations such as by Knighton (2014); Chang (1992).

With the aid of the regime equations such as those in Eq. (12), quantitative analysis that shows the effects of variation of more than a single variable could be done as follows. First, the discharge *Q* and the width *B* are assumed as the only variables while roughness and depth are assumed constants. A value of b equal to 0.5 is assumed in Eq. (12), i.e., $\Delta Q/Q = 0.5\ \Delta B/B$ which is substituted into Eq. (34) resulting in:

$$\frac{\Delta\lambda}{\lambda} = \frac{\Delta r}{r} = \left\{\frac{\Delta Q}{Q} - 0.5\ \frac{\Delta Q}{Q}\right\} = 0.5\ \frac{\Delta Q}{Q} \tag{67}$$

Equation (67) indicates that when the channel width increases due to increase in the discharge, the radius of curvature is proportional to the width. In that case, small width channels are more meandering while wider channels tend toward straight and cutoff condition. This last case is in contrast to the case of changing width only that was discussed above which highlights the difference in considering single and combined variables. Equation (67) also indicates that $\lambda \propto Q^{0.5}$ which is supported in that Dury (1964) reports $\lambda \propto Q^{0.5}$, Carlston (1965) reports: $\lambda \propto Q^{0.46}$ and Ackers *et al*. (1970) reports $\lambda \propto Q^{0.47}$. As ΔQ/Q = 2 ΔB/B, Eq. (67) indicates that:

$$\frac{\Delta\lambda}{\lambda} = \frac{\Delta B}{B}\ ;\ or\ \lambda \propto B \tag{68}$$

The relation $\lambda \propto B$ is in line with Yalin (1971) hypothesis that $\lambda = 2\,\pi\,B$.

In a similar fashion when assuming the discharge and depth are only varying, with a depth exponent f = 1/3, this results in that $\Delta\lambda/\lambda = (2/3)\ \Delta Q/Q\ ;\ or\ \lambda \propto Q^{2/3}$.

If the discharge, width and depth vary while *b* = 0.5 and $f = 1/3$, this results in that: $\Delta\lambda/\lambda = (1/6)\ \Delta Q/Q\ ;\ or\ \lambda \propto Q^{1/6}$. In summary, there is no unique constant relation between the meander wave length and discharge or width and the variation of the meander wavelength depends on the number of controlling variables (e.g., *Q*, *B*, *D* and *C*) and the intensity and magnitude of their variation.

It should be noted that in Eqs. (4 and 5) linear perturbation was applied, however, in the present approach nonlinear perturbation starting from quadratic perturbation is possible in principle but the mathematics involved will be more complex, so it is left for future research.

It should be noted that in the case of the Nile River in Egypt, it was assumed that the relation $\lambda = 6\,B$ is valid for the pre-AHD conditions. However, other researchers had different form such as Richards (1982), who performed regression analysis between wavelength and channel width in the literature and found that $\lambda = 12.34\,B$ or simply: $\lambda = 12\,B$. In addition, the roughness term was neglected. The two assumptions made before that $\lambda = 6\,B$ and neglecting roughness effects are replaced herein by another two assumptions which are that $\lambda = 12\,B$ and existence of roughness. It can be argued that the pre-AHD Nile was in a natural state during the flood season as all barrage gates were open. However, the post-AHD Nile has the barrage gates partially closed all over the year and the flood water and sediment are stored in the AHD's lake making the flow regime of the post-AHD Nile regulated by passing from the dam only the needed water for generating electricity, agricultural, industrial and domestic water requirements. Thus there is no assurance that if the relation $\lambda = 6\,B$ is valid for the post-AHD that it should also be valid under pre-AHD conditions as the river flow and sediment regimes differ in both cases. Regarding roughness it is assumed that its effect exist but due to lack of data it will be assumed that the roughness term offsets the width and depth terms leaving only the discharge term. In this case Eq. (34), which assumes minimum transverse energy loss slope, becomes:

$$\frac{\Delta\lambda}{\lambda} = \frac{\Delta Q}{Q} \tag{69}$$

Or:

$$\lambda_2 = \left(1 + \frac{\Delta Q}{Q}\right)\lambda_1 \tag{70}$$

For the third reach $\lambda_1 = 12\,B_1 = 12\,(924) = 11088$ m and ΔQ/Q as before is -0.724. Upon substitution of these values into Eq. (70) it results in value of predicted λ_2 = 3063 m while the measured value is 3000 m making an excellent agreement.

For the fourth reach, $\lambda_1 = 12\,B_1 = 12\,(1025) = 12300$ m and $\Delta Q/Q$ as before is -0.774. Upon substitution of these values into Eq. (70) it results in value of predicted λ_2 = 2829 m while the measured value is 2830 m making again an excellent agreement.

DOI: 10.3844/ajessp.2025.12.38

The last two examples improved significantly the performance of Eq. (34) in the third and fourth reaches where the ratio of computed to measured wave length is almost 1.0 while it was before1.62 and 1.94 as seen in Table (5). Now a question arises as which assumptions should be followed? The answer is simple which is that in real-life applications data often exist and through which some sort of calibration process will determine which concept is more appropriate, i.e. whether it is the minimum transverse energy loss slope or transverse stream power and also which terms and coefficients should be adopted as seen also in the case of the four USA Rivers. Due to lack of some data in the case of the Nile River some assumptions had to be made.

The present approach theoretical developed equations (e.g., Eqs. (27, 34-35)) can all be cast in the following general form as:

$$\frac{\Delta r}{r} = \frac{\Delta \lambda}{\lambda} = \left\{ a_C \, \Delta C + a_Q \, \frac{\Delta Q}{Q} + a_B \, \frac{\Delta B}{B} + a_D \, \frac{\Delta D}{D} \right\} \qquad (71)$$

where, the a's are coefficients which could be determined through multiple regressions using field data. In doing so, the theoretical approach could be thus converted into a semi-empirical approach based on field data. Although the analytical model was applied for a long term river meandering changes either at the Nile River in Egypt or the four USA Rivers in Texas, it could also be applied for short transient changes as seen in Eq. (40).

Table (7) shows prediction of seven cases at the four USA Rivers (Texas) in which channel width increased or decreased and so did the radius of curvature. Table (7) shows successful predictions by the present approach, Eq. (60), while Briaud *et al.* (2001) predictions are in less agreement with the data although they reported success in prediction of the radius of curvature. The large errors associated with the sequence maps and extrapolation method is attributed mainly to the assumption of a constant meander migration rate (dR/dt).

In the cases shown in Table (8) it is noted that the relative change in the radius of curvature ($\Delta r/r$) is almost twice as the relative change in the channel width ($\Delta B/B$) and both have the same trend of the direction of change whether a decrease or increase. Case (1) at the Brazos River spanned 78 years in which the channel radius of curvature decreased from 600 to 453 m then increased to 558 m and these changes are well captured by Eq. (60) of the present approach. Because Briaud *et al.* (2001) approach has to use two field data sets (1910 and 1958 in this case) it had to start predictions afterward starting from the year 1981. Although their method of sequence maps and extrapolation is based on using actual measured data their prediction were not that accurate compared to Eq. (60) not only in magnitude (one prediction had error in *r* of 150 m and another 77 m) but also in direction of change as the radius of curvature predicted by them to have a decreasing trend between the years 1981 and 1988 in contrary to the measured data which showed increasing trend. The concept of minimum transverse stream power as represented by Eq. (60) succeeded in all of the seven cases with excellent agreement with the data and the assumption that b = 0.5 worked out well. Mathematically speaking the present approach developed equations, due to the linearization process, should have the variables change over a short period of time and is therefore suitable for short time transient analyses. However, the method worked very well for very long term predictions such as from 1910-1958 at the Brazos River (i.e., 48 years). This is could be justified by that river responses could have a long time scale as far as changes are concerned.

As can be seen in Table (8), the special cases in the four USA Rivers in Texas have either of: The direction of channel radius of curvature change is in reverse to the direction of width change or that the magnitude of the relative width change ($\Delta B/B$) is much more than the relative change in the radius of curvature ($\Delta r/r$). Of course, these unusual conditions require special treatments as can be seen in the assumptions listed in Table (8). As the magnitude of width change is high in almost all cases it was natural that the width exponent (b) to have values higher than b = 0.5 which was taken in the previous regular cases. For example, the width exponent b took values of 0.75, 1.0, 1.16 and 1.5. In five cases the minimum transverse energy slope loss equation was assumed applicable while in two cases the minimum transverse stream power assumed applicable. Both of the current approach and the method of sequence maps and extrapolation adopted by Briaud *et al.* (2001) used calibration process, however, the present approach predictions are far more superior and in excellent agreement with the field data. It is worth mentioning here that Ashraf and Liu (2013) applied Ikeda *et al.* (1981) meander migration model to three of the four rivers discussed here, namely: Brazos River, Nueces River and Trinity River and had difficulty in their calibration process. As stated earlier, for the Nueces River at the U.S. 90 crossing, the prediction error ranged from 29.51-91.58 m, for the Brazos River (S.H. 105 Bridge) it ranged from 39.28-41.85 m and for the Trinity River (F.M. 787 Bridge) it ranged from 42.38 to 84.11 m. Indeed these errors are very high for a calibration process.

It can be stated therefore that predictions by the present approach theory is far more superior than both of Ikeda *et al.* (1981) meander migration model and the sequence maps and extrapolation method by (Brice, 1982); Lagasse 2001). This is in spite that the present approach is theoretical and in case of using a calibration process it demands much less data than these two other methods. The field cases discussed here especially the USA Rivers point out to an important issue which is that width changes have a very direct impact on river meander migration and

DOI: 10.3844/ajessp.2025.12.38

changes in the channel radius of curvature. This is due to the link between width changes and bank resistivity and that also width reflects the stream size and could be a surrogate to discharge. However, this is so due to lack of data for other variables such as channel depth and roughness as pointed out by Hafez (2022) who showed the necessity of having all the controlling variables in addition to the width in order to obtain a complete and reliable analysis and successful predictions. Indeed having hydraulic and roughness data in addition to the geometric data, that has to be more complete and inclusive of all the relevant variables, will aid in more testing of the proposed approach and gives more insight into the mechanics of meander migration.

Now an alternative equation to Eq. (46) is presented for determining the change in the angle θ based on the concept of extremal channel sinuosity. Channel sinuosity is given by Hafez (2022) based on the excess energy theory as:

$$\Omega = 1 + \left(\frac{\mathrm{D}}{\mathrm{r}}\right)^2 F_r^2 \frac{1}{\mathrm{S_R}} \Phi(\mathrm{C}) \tag{72}$$

where, Ω is the channel sinuosity and S_R is the river channel regime slope, i.e., the equilibrium channel slope (e.g., given as in Eq. (78 or 81) thereafter). For very large r values, Ω approaches unity which is the value of a straight channel path. Therefore, Eq. (72) has a minimum value of unity and because of its nonlinear character it is expected to have a maximum value dictated by the relative magnitude of the variables appearing in the equation. Thus, Eq. (72) could have both of a maximum and minimum, i.e., at extremum or having extremal conditions. The quantity (Ω -1) could be considered as the excess sinuosity in which a straight line or path would have a zero value.

At extremal channel sinuosity ΔΩ/Ω = 0 or alternatively Δ(Ω-1) / (Ω - 1) = 0. Applying this condition to Eq. (72) yields:

$$2\,\frac{\Delta D}{D} - 2\,\frac{\Delta r}{r} + 2\,\frac{\Delta F_r}{F_r} - \frac{\Delta S_R}{S_R} - \Psi(C)\frac{\Delta C}{C} = 0 \tag{73}$$

Substituting Δr/r from Eq. (42) into Eq. (73) yields:

$$2\,\frac{\Delta D}{D} - 2\,(\frac{\Delta L}{L} - \frac{\Delta \theta}{\theta}) + 2\,\frac{\Delta F_r}{F_r} - \frac{\Delta S_R}{S_R} - \Psi(C)\frac{\Delta C}{C} = 0 \tag{74}$$

Solving for Δθ/θ in Eq. (74) results in:

$$\frac{\Delta \theta}{\theta} = -\frac{\Delta D}{D} + \frac{\Delta L}{L} - \frac{\Delta F_r}{F_r} + \frac{1}{2}\frac{\Delta S_R}{S_R} + \frac{1}{2}\Psi(C)\frac{\Delta C}{C} \tag{75}$$

Substituting ΔL/L from Eq. (45) into Eq. (75) yields:

$$\frac{\Delta \theta}{\theta} = -0.45\,\frac{\Delta f}{f} - \frac{\Delta F_r}{F_r} + \frac{1}{2}\frac{\Delta S_R}{S_R} + \frac{1}{2}\Psi(C)\frac{\Delta C}{C} \tag{76}$$

Applying the differential operator as in Eq. (5) to the Froude number in Eq. (22) and substituting the resulting expression into Eq. (76) yields:

$$\frac{\Delta \theta}{\theta} = \frac{\Delta B}{B} + \frac{3}{2}\frac{\Delta D}{D} - \frac{\Delta Q}{Q} - 0.45\,\frac{\Delta f}{f} + \frac{1}{2}\frac{\Delta S_R}{S_R} + \frac{1}{2}\Psi(C)\frac{\Delta C}{C} \tag{77}$$

The relative change in the regime channel slope could be given using Lacey (1958) equation which reads as:

$$\mathrm{S_R} = \frac{(1.6\, d_m^{1/2})^{5/3}}{1830\, \mathrm{Q}^{1/6}} \tag{78}$$

where, d_m is the median bed-material size in millimeters and Q is the flow discharge (cfs).

Applying the differential operator as in Eq. (5) to Eq. (78) yields:

$$\frac{\Delta S_R}{S_R} = \frac{5}{16}\frac{\Delta d_m}{d_m} - \frac{1}{6}\frac{\Delta Q}{Q} \tag{79}$$

Substituting Eq. (79) into Eq. (77) gives the final equation for the change in θ as:

$$\frac{\Delta \theta}{\theta} = \frac{\Delta B}{B} + \frac{3}{2}\frac{\Delta D}{D} - \frac{13}{12}\frac{\Delta Q}{Q} - 0.45\,\frac{\Delta f}{f} + \frac{5}{32}\frac{\Delta d_m}{d_m} + \frac{1}{2}\Psi(C)\frac{\Delta C}{C} \tag{80}$$

Hafez (2022) presents an alternative equation for S_R as:

$$S_R = \frac{\tau_c \pm \sqrt{\tau_c{}^2 + 4\left(\frac{d_m^{4/3}\, q_s}{0.173}\right)}}{2\gamma R} \tag{81}$$

where, τ_c is the critical shear stress for incipient motion, q_s is the unit bed load discharge, d_m is the median bed size in mm, γ is the water unit weight and R is the channel hydraulic radius (equals the water depth D for very wide channels). Equation (81) has much more complex structure than Eq. (78) making its use a little harder.

Equation (80) expresses the change in the angle θ in terms of changes in the channel width, depth, flow, median bed material size and roughness. Unfortunately, it is hard to find data to test Eq. (80) even qualitatively as past studies do not focus on changes in the angle θ. It is noted that the approach used to derive Eq. (80) combined the geometrical constrain between r and θ as given by Eq. (42), the sinuosity equation as given by the excess energy theory, the meander path arc length based on data and finally the extremal hypothesis of extremal channel sinuosity. Such a collection reflects the complexity of the process of river migration dynamics. Note that extremal condition means either minimum or maximum which is the case for channel sinuosity function which could attain both of minimum and maximum. As channel sinuosity is defined as valley slope over channel slope, its use here include the effect of the valley slope which represents the geological conditions of meander formation. According to

DOI: 10.3844/ajessp.2025.12.38

Mackin (1963), any account of winding (meandering) rivers in terms of the slope of a valley floor or other surface leaves out a factor that would be very important to a geologist: The origin of that valley floor or surface. Evolving, mobile rivers, as opposed to quasistatic channelized flows, create the valley floors and surfaces upon which they flow at any moment in time. From this geological viewpoint, an explanation for the pattern of any evolving river must include something about the historical development of that river, (Baker, 2013). Therefore, inclusion of the excess energy theory equation which considers valley slope supports the arguments by Mackin (1963); Baker (2013).

Bed aggradation/degradation effects can be included via the change in the depth term as follows. The channel flow depth (D) could be written as $D = Z_w - Z_b$, where Z_w is water surface elevation while Z_b is the bed elevation in an average sense. Performing incremental differentiation as in Eq. (5) on this relation yields:

$$\frac{\Delta D}{D} = \frac{\Delta Z_w}{Z_w} - \frac{\Delta Z_b}{Z_b} \tag{82}$$

The change in the bed level could be given such as by the Exner equation as:

$$(1-e)\,\frac{\Delta Z_b}{\Delta t} + \frac{\Delta q_s}{\Delta s} = 0 \tag{83}$$

Or:

$$\Delta Z_b = -\frac{1}{(1-e)}\,\frac{\Delta t}{\Delta s}\,\Delta q_s \tag{84}$$

where, e is the porosity of the bed layer, t is time (T), q_s is the unit bed load rate (L^2/T), s is stream-wise coordinate (L), T is a time dimension and L is a length dimension. In this way imbalances of the sediment load leads to bed rising/lowering or bed aggradation/degradation; and through substituting Eq. (84) into Eq. (82) sediment changes are affecting meander migration process.

It can be stated that the change in the radius of curvature (r) affects the lateral extent of the meander bend while the change in θ affects the bend upstream and downstream movements and skewness. Support to the hypothesis of extremal channel sinuosity could be given in the finding by Guo *et al*. (2019) that the field data suggest that meander bends without external forcing such as engineering works tend to evolve from downstream-skewed low-sinuosity bends to upstream-skewed high-sinuosity bends before cutoff. They further add that how skewing evolves as bends develop remains incompletely understood. Their analysis shows that, on 20 reaches of nearly pristine alluvial meandering rivers, downstream skewing dominates when the bends are relatively straight, but upstream skewing increasingly dominates as bend sinuosity increases. Equation (80) which could predict upstream and downstream skewness based on extremal sinuosity could be helpful in such type of analyses.

Now, both of Eq. (40 and 80) offer a complete description of the movement of a point located on the river channel centreline in a two-dimensional horizontal plane. As pointed out before that theoretical work should furnish the floor and precede field and experimental data collection, therefore Eq. (40 and 80) give a useful guideline for the type of data collection which is important for investigating meandering river migration dynamics.

The suggested approach could be considered as a generalization in time of Ikeda *et al*. (1981) seminal excess velocity bank erosion model, or to the excess shear stress model and also a generalization of the geomorphic regime theory equations.

Conclusion

In conclusion, we have demonstrated the conceptual development of a dynamic model for meander migration that provides two equations to describe the movement of a point on a river axis in a two-dimensional horizontal plane (r, θ) or (x, y). The model is based on the fundamental assumption that lateral meander migration can be attributed to the minimization of transverse energy loss slope or transverse stream power, while downstream/upstream bend migration is influenced by extremal channel sinuosity. Building upon the extremal technique introduced by Hafez (2000) for straight river reaches, we have successfully extended the theory to curved meandering river reaches.

By applying a differential increment technique or linear perturbation to the equations of transverse energy loss slope or transverse stream power, we obtained an equation that describes the incremental change in the channel radius of curvature. This equation incorporates variations in flow discharge, flow width, flow depth and channel roughness, linking all the controlling variables of the meander migration process. Furthermore, the equation can be used to determine the relative change in meander wavelength. We also applied the differential incremental operator to the developed equation for channel sinuosity and meander bend arc length, as established by Hafez (2022), resulting in an equation for the relative change in the arc angle.

The proposed model allows for the determination of critical flow discharge for incipient meander-neck-cutoff and chute cutoff, employing a methodology similar to the energy balance theory developed for scour analysis by Hafez (2016a). The flexibility of the model equations enables their integration with regime theory equations that relate channel variables to flow discharge. While the model equations can be considered a generalization of Ikeda *et al*. (1981) meander migration model, based on

excess bank velocity or excess bank shear stress, this generalization is primarily from a temporal perspective rather than spatiality.

One of the key advantages of the analytical model is its simplicity and ease of application, eliminating the need for complex computer programming. It can accommodate spatial and temporal variations in lateral meander movement, offering a comprehensive analysis. The model's equations have demonstrated their predictive capability, successfully estimating the thalweg wavelength at the Nile River in Egypt and accurately predicting changes in the river channel radius of curvature for four rivers in Texas, USA. These predictions outperformed those made using Ikeda *et al*. (1981) meander migration model, as well as the sequence maps and extrapolation method proposed by Brice (1982); Lagasse (2001).

This study emphasizes the importance of collecting hydraulic and roughness data, in addition to geometric data acquired through remote sensing, for a thorough analysis of meander migration. By incorporating these comprehensive datasets, a more complete understanding of the process can be achieved, leading to improved predictions and management strategies.

Acknowledgment

The author would like to present his sincere gratitude and appreciation to anonymous reviewers for the very fruitful, informative and important remarks, suggestions and comments which really helped in the significant improving of this manuscript. Special appreciations go to Prof. Dr. Hossam El-Sersawy and Dr. Fatma Saad at the Nile Research Institute, Egypt.

Funding Information

This study has not received any funding.

Ethics

The author declares that he has no known competing financial interests or personal relationships that could have appeared to influence the work reported in this study and that this study adheres to ethics.

References

Abad, J. D., & Garcia, M. H. (2006). Rvr Meander: A Toolbox for Re-Meandering of Channelized Streams. *Computers & Geosciences*, *32*(1), 92–101. https://doi.org/10.1016/j.cageo.2005.05.006

Ackers, P., Charlton, F., & HRS. (1970). Summary of Paper 7362. The Slope and Resistance of Small Meandering Channels. *Proceedings of the Institution of Civil Engineers*, *47*(3), 388. https://doi.org/10.1680/iicep.1970.6579

Ashraf, F. U., & Liu, X. (2013). River Meandering Prediction: Case Studies for Four Rivers in Texas. *World Environmental and Water Resources Congress 2013*, 2009–2019. https://doi.org/10.1061/9780784412947.197

Baker, V. R. (2013). Sinuous Rivers. *Proceedings of the National Academy of Sciences*, *110*(21), 8321–8322. https://doi.org/10.1073/pnas.1306619110

Blanckaert, K. (2011). Hydrodynamic Processes in Sharp Meander Bends and their Morphological Implications. *Journal of Geophysical Research: Earth Surface*, *116*(F1). https://doi.org/10.1029/2010jf001806

Blench, T. (1952). Regime Theory for Self-Formed Sediment-Bearing Channels. *Transactions of the American Society of Civil Engineers*, *117*(1), 383–400. https://doi.org/10.1061/taceat.0006641

Blench, T. (1970). Regime Theory Design of Canals with Sand Beds. *Journal of the Irrigation and Drainage Division*, *96*(2), 205–213. https://doi.org/10.1061/jrcea4.0000718

Bogoni, M., Putti, M., & Lanzoni, S. (2017). Modeling Meander Morphodynamics Over Self-Formed Heterogeneous Floodplains. *Water Resources Research*, *53*(6), 5137–5157. https://doi.org/10.1002/2017wr020726

Briaud, J.-L., Chen, H.-C., & Park, S. (2001). *Predicting Meander Migration: Evaluation of Some Existing Techniques.* Texas Transportation Institute the Texas A&M University System.

Brice, J. C. (1982). *Stream Channel Stability Assessment*. Federal Highway Administration.

Bridge, J. S. (1977). Flow, bed topography, grain size and sedimentary structure in open channel bends: A three-dimensional model. *Earth Surface Processes*, *2*(4), 401–416. https://doi.org/10.1002/esp.3290020410

Camporeale, C., Perona, P., Porporato, A., & Ridolfi, L. (2007). Hierarchy of Models for Meandering Rivers and Related Morphodynamic Processes. *Reviews of Geophysics*, *45*(1). https://doi.org/10.1029/2005rg000185

Carlston, C. W. (1965). The Relation of Free Meander Geometry to Stream Discharge and its Geomorphic Implications. *American Journal of Science*, *263*(10), 864–885. https://doi.org/10.2475/ajs.263.10.864

Chang, H. H. (1984). Regular Meander Path Model. *Journal of Hydraulic Engineering*, *110*(10), 1398–1411. https://doi.org/10.1061/(asce)0733-9429(1984)110:10(1398)

Chang, H. H. (1992). *Fluvial Processes in River Engineering*. Wiley-Interscience.

Constantine, J. A., McLean, Stephen R., & Dunne, T. (2010). A Mechanism of Chute Cutoff along Large Meandering Rivers with Uniform Floodplain Topography. *Geological Society of America Bulletin*, *122*(5–6), 855–869. https://doi.org/10.1130/b26560.1

Crosato, A. (2007). Effects of Smoothing and Regridding in Numerical Meander Migration Models. *Water Resources Research*, *43*(1). https://doi.org/10.1029/2006wr005087

Da Silva, A. M. F. (2006). On why and how do rivers meander. *Journal of Hydraulic Research*, *44*(5), 579–590. https://doi.org/10.1080/00221686.2006.9521708

Dury, G. H. (1964). *Principles of Underfit Streams*.

Dury, G. H. (1976). Discharge Prediction, Present and Former, from Channel Dimensions. *Journal of Hydrology*, *30*(3), 219–245. https://doi.org/10.1016/0022-1694(76)90102-5

Eke, E. C., Czapiga, M. J., Viparelli, E., Shimizu, Y., Imran, J., Sun, T., & Parker, G. (2014). Coevolution of width and Sinuosity in Meandering Rivers. *Journal of Fluid Mechanics*, *760*, 127–174. https://doi.org/10.1017/jfm.2014.556

Ferreira da Silva, A. M., & Ebrahimi, M. (2017). Meandering Morphodynamics: Insights from Laboratory and Numerical Experiments and Beyond. *Journal of Hydraulic Engineering*, *143*(9), 03117005. https://doi.org/10.1061/(asce)hy.1943-7900.0001324

Finotello, A., D'Alpaos, A., Bogoni, M., Ghinassi, M., & Lanzoni, S. (2020). Remotely-Sensed Planform Morphologies Reveal Fluvial and Tidal Nature of Meandering Channels. *Scientific Reports*, *10*(1), 54. https://doi.org/10.1038/s41598-019-56992-w

Frascati, A., & Lanzoni, S. (2009). Morphodynamic Regime and Long-Term Evolution of Meandering Rivers. *Journal of Geophysical Research: Earth Surface*, *114*(F2). https://doi.org/10.1029/2008jf001101

Guo, X., Chen, D., & Parker, G. (2019). Flow Directionality of Pristine Meandering Rivers is Embedded in the Skewing of High-Amplitude Bends and Neck Cutoffs. *Proceedings of the National Academy of Sciences*, *116*(47), 23448–23454. https://doi.org/10.1073/pnas.1910874116

Hafez, Y. (2002). On the Dynamic Adjustments of Stream Channels. *Journal of Environmental Hydrology, International Association for Environmental Hydrology*, *10*. https://doi.org/10.13140/RG.2.2.13262.06727

Hafez, Y. I. (2000). Response Theory for Alluvial River Adjustments to Environmental and Man-made Changes "Journal of Environmental Hydrology. *Journal of Environmental Hydrology*, *8*.

Hafez, Y. I. (2001a). New Concepts for Alluvial River Response to Change in Regime. *World Water & Environmental Resources Congress*, 1–10. https://doi.org/10.1061/40569(2001)46

Hafez, Y. I. (2001b). River Response to Sediment Load, World Water & Environmental Resources Congress. *Meeting the World's Water and Environmental Resources Challenges*, 1–10.

Hafez, Y. I. (2016a). Mathematical Modeling of Local Scour at Slender and Wide Bridge Piers. *Journal of Fluids*, *2016*, 1–19. https://doi.org/10.1155/2016/4835253

Hafez, Y. I. (2016b). Scour due to Turbulent Wall Jets Downstream of Low-/High-Head Hydraulic Structures. *Cogent Engineering*, *3*(1), 1200836. https://doi.org/10.1080/23311916.2016.1200836

Hafez, Y. I. (2018). Three Dimensional Mathematical Modeling of Plunge Pool Scour. *MOJ Civil Engineering*, *4*(4), 192–204. https://doi.org/10.15406/mojce.2018.04.00119

Hafez, Y. I. (2022). Excess energy theory for river curvature and meandering. *Journal of Hydrology*, *608*, 127604. https://doi.org/10.1016/j.jhydrol.2022.127604

Hafez, Y.I. (1995). *A k-e Turbulence Model for Predicting the Three-Dimensional Velocity Field and Boundary Shear in Open and Closed Channels"*.

Hayashi, T. (1971). Study of the Cause of Meanders. *Trans. JSCE*, *2*.

Hooke, J. M. (1980). Magnitude and Distribution of Rates of River Bank Erosion. *Earth Surface Processes*, *5*(2), 143–157. https://doi.org/10.1002/esp.3760050205

Hooke, J. M. (2004). Cutoffs Galore!: Occurrence and Causes of Multiple Cutoffs on a Meandering River. *Geomorphology*, *61*(3–4), 225–238. https://doi.org/10.1016/j.geomorph.2003.12.006

Howard, A. D., & Hemberger, A. T. (1991). Multivariate Characterization of Meandering. *Geomorphology*, *4*(3–4), 161–186. https://doi.org/10.1016/0169-555x(91)90002-r

Howard, A. D., & Knutson, T. R. (1984). Sufficient Conditions for River Meandering: A Simulation Approach. *Water Resources Research*, *20*(11), 1659–1667. https://doi.org/10.1029/wr020i011p01659

Ielpi, A., Lapôtre, M. G. A., Finotello, A., & Ghinassi, M. (2021). Planform-Asymmetry and Backwater Effects on River-Cutoff Kinematics and Clustering. *Earth Surface Processes and Landforms*, *46*(2), 357–370. https://doi.org/10.1002/esp.5029

Ikeda, S., Parker, G., & Sawai, K. (1981). Bend Theory of River Meanders. Part 1. Linear Development. *Journal of Fluid Mechanics*, *112*, 363–377. https://doi.org/10.1017/s0022112081000451

Keady, P. D., & Priest, M. S. (1977). The Downstream Migration Rate of River Meandering Patterns. *Mississippi Water Resources Conference, Meeting 12th Mississippi Water Resources Conference, Jackson, MS*, 29–34.

Knighton, D. (2014). *Fluvial Forms and Proesses* (2nd Ed.). Routledge. https://doi.org/10.4324/9780203784662

Lacey, G. (1930). Stable Channel in Alluvium. *Proc. Inst. Civ*.

Lacey, G. (1958). Uniform Flow in Alluvial Rivers and Canals, Proc. *Inst. Civ. Eng., London*, 11.

Lagasse, P. (2001). *Personal Communication with Briaud*.

Langbein, W. B., & Leopold, L. B. (1966). River Meanders-Theory of Minimum Variance. *USGS Professional Paper*, 422.

Leopold, L. B., & Langbein, W. B. (1966). River Meanders. In *Scientific American* (Vol. 214, Issue 6, pp. 60–70). https://doi.org/10.1038/scientificamerican0666-60

Leopold, L. B., & Maddock, T. (1953). *The Hydraulic Geometry of Stream Channels and Some Physiographic Implications*. *252*.

Leopold, L. B., & Wolman, M. G. (1957). *River Channel Patterns: Braided, Meandering and Straight*. https://doi.org/doi.org/10.3133/pp282B

Leopold, L. b., & Wolman, M. G. (1960). River Meanders. In *Geological Society of America Bulletin* (Vol. 71, Issue 6, pp. 769–793). https://doi.org/10.1130/0016-7606(1960)71[769:rm]2.0.co;2

Mackin, J. H. (1963). *Rational and empirical methods of investigation in geology*.

Monegaglia, F., & Tubino, M. (2019). The Hydraulic Geometry of Evolving Meandering Rivers. In *Journal of Geophysical Research: Earth Surface* (Vol. 124, Issue 11, pp. 2723–2748). https://doi.org/10.1029/2019jf005309

Nanson, G. C., & Hickin, E. J. (1983). Channel Migration and Incision on the Beatton River. In *Journal of Hydraulic Engineering* (Vol. 109, Issue 3, pp. 327–337). https://doi.org/10.1061/(asce)0733-9429(1983)109:3(327)

NRI. (1992). *Nile Research Institute, River Regime of the Nile in Egypt*.

Odgaard, A. J. (1986). Meander Flow Model. I: Development. In *Journal of Hydraulic Engineering* (Vol. 112, Issue 12, pp. 1117–1135). https://doi.org/10.1061/(asce)0733-9429(1986)112:12(1117)

Parker, G., Shimizu, Y., Wilkerson, G. V., Eke, E. C., Abad, J. D., Lauer, J. W., Paola, C., Dietrich, W. E., & Voller, V. R. (2011). A new Framework for Modeling the Migration of Meandering Rivers. In *Earth Surface Processes and Landforms* (Vol. 36, Issue 1, pp. 70–86). https://doi.org/10.1002/esp.2113

Pittaluga, M. B., & Seminara, G. (2011). Nonlinearity and Unsteadiness in River Meandering: A Review of Progress in Theory and Modelling. *Earth Surface Processes and Landforms*, *36*(1), 20–38. https://doi.org/10.1002/esp.2089

Richards, K. (1982). *Rivers: form and Process in Alluvial Channels*. *9*.

Rozovskii, I. L. (1957). *Flow of Water in Bends of Open Channels*

Schwenk, J., Lanzoni, S., & Foufoula-Georgiou, E. (2015). The Life of a Meander Bend: Connecting Shape and Dynamics Via Analysis of a Numerical Model. In *Journal of Geophysical Research: Earth Surface* (Vol. 120, Issue 4, pp. 690–710). https://doi.org/10.1002/2014jf003252

Seminara, G. (2006). Meanders. *Journal of Fluid Mechanics*, *554*, 271–297. https://doi.org/10.1017/S0022112006008925

Seminara, G., Zolezzi, G., Tubino, M., & Zardi, D. (2001). Downstream and Upstream Influence in River Meandering. Part 2. Planimetric Development. *Journal of Fluid Mechanics*, *438*, 213–230. https://doi.org/10.1017/s0022112001004281

Simons, D. B., & Albertson, M. L. (1960). Uniform Water Conveyance Channels in Alluvial Material. In *Journal of the Hydraulics Division* (Vol. 86, Issue 5, pp. 33–71). https://doi.org/10.1061/jyceaj.0000478

Sylvester, Z., Durkin, P., & Covault, J. A. (2019). High Curvatures Drive River Meandering. *Geology*, *47*(3), 263–266. https://doi.org/10.1130/g45608.1

Task Committee on the Bed Configura. (1973). the Bed Configuration and Roughness of Alluvial Streams. In *Proceedings of the Japan Society of Civil Engineers* (Vol. 1973, Issue 210, pp. 65–91). https://doi.org/10.2208/jscej1969.1973.210_65

van Dijk, W. M., van de Lageweg, W. I., & Kleinhans, M. G. (2012). Experimental Meandering River with Chute Cutoffs. *Journal of Geophysical Research: Earth Surface*, *117*(F3). https://doi.org/10.1029/2011jf002314

Weiss, S. F., & Higdon, J. J. L. (2022). Dynamics of meandering rivers in finite-length channels: linear theory. In *Journal of Fluid Mechanics* (Vol. 938, p. A11). https://doi.org/10.1017/jfm.2022.131

Williams, G. P. (1978). *Hydraulic Geometry of River Cross Sections geol*. *1029*.

Wu, X., Hu, X., & Zhang, X. (2023). Experimental Study on Neck Cutoff in Meandering River under Variable Discharges. *Water*, *15*(5), 841–999. https://doi.org/10.3390/w15050841

Yalin, M. S. (1971). On the Formation of Dunes and Meanders. *Proceedings of the 14th International Congress of the Hydraulic Research Association*, 1–8.

Yalin, M. S. (1992). *River Mechanics"*. https://doi.org/10.1016/B978-0-08-040190-4.50006-X

Yalin, M. S., & Silva, A. M. F. (2001). *Fluvial Processes"*.

Yang, C. T. (1986). Dynamic Adjustment of Rivers. *Third International Symposium on River Sedimentation*. Third International Symposium on River Sedimentation.

Yang, C. T., Song, C. C. S., & Woldenberg, M. J. (1981). Hydraulic Geometry and Minimum Rate of Energy Dissipation. *Water Resources Research*, *17*(4), 1014–1018. https://doi.org/10.1029/wr017i004p01014

Zhao, K., Lanzoni, S., Gong, Z., & Coco, G. (2021). A Numerical Model of Bank Collapse and River Meandering. *Geophysical Research Letters*, *48*(12), e2021GL093516. https://doi.org/10.1029/2021gl093516

Zolezzi, G., Luchi, R., & Tubino, M. (2009). Morphodynamic Regime of Gravel Bed, Single-Thread Meandering Rivers. *Journal of Geophysical Research: Earth Surface*, *114*(F1). https://doi.org/10.1029/2007jf000968